

# Lorentz-violating wormholes: The role of the matter coupled to Lorentz-violating fields

Renan B. Magalhães<sup>a</sup> Leandro A. Lessa<sup>a</sup> Rodolfo Casana<sup>a,b</sup>

<sup>a</sup>Programa de Pós-graduação em Física, Universidade Federal do Maranhão, Campus Universitário do Bacanga, São Luís (MA), 65080-805, Brazil.

<sup>b</sup>Departamento de Física, Universidade Federal do Maranhão, Campus Universitário do Bacanga, São Luís, Maranhão 65080-805, Brazil.

E-mail: [renan.batalha@ufma.br](mailto:renan.batalha@ufma.br), [leandrophys@gmail.com](mailto:leandrophys@gmail.com), [rodolfo.casana@ufma.br](mailto:rodolfo.casana@ufma.br)

**Abstract.** The anisotropies induced by Lorentz-violating fields pose significant challenges for the search for compact objects in non-vacuum environments. In this work, we demonstrate that introducing couplings between Lorentz-violating fields and matter facilitates the formation of traversable wormholes. Specifically, we introduce additional couplings in the Lagrangian of a phantom scalar field and derive Ellis-Bronnikov spacetime analogs in three distinct Lorentz-violating scenarios: (I) modifications arising from the vacuum expectation value of the bumblebee field, (II) contributions from the vacuum expectation value of an antisymmetric rank-2 tensor field, and (III) a combined scenario incorporating both fields. In the latter case, despite the distinct nature of the fields, their non-zero vacuum expectation values contribute additively to the overall effect on the phantom distribution and on the resulting line element. Moreover, we consider scalar waves to probe the effects of the Lorentz violation in these spacetimes. Notably, the additional Lorentz-violating couplings can alter scalar field dynamics such that perturbations propagate as if in a General Relativity background, which allows for some traits of Lorentz violation to be hidden. We compute the quasinormal mode spectra of these perturbations using three methods: direct integration, 6th-order WKB approximation, and the Prony method, finding strong agreement among the results.

---

## Contents

<b>1</b>	<b>Introduction</b>	<b>1</b>
<b>2</b>	<b>Framework</b>	<b>3</b>
<b>3</b>	<b>Wormholes supported by phantom distributions coupled to Lorentz-violating fields</b>	<b>6</b>
3.1	Case I: vector (bumblebee)	8
3.2	Case II: antisymmetric rank-2 tensor	9
3.3	Case III: vector and antisymmetric rank-2 tensor	10
<b>4</b>	<b>Dynamics of scalar perturbations in Lorentz-violating wormholes</b>	<b>11</b>
4.1	Effective potential	14
<b>5</b>	<b>Quasinormal frequencies</b>	<b>15</b>
<b>6</b>	<b>A note on scalar perturbations subjected to couplings to Lorentz-violating fields</b>	<b>19</b>
<b>7</b>	<b>Conclusion</b>	<b>23</b>
<b>A</b>	<b>Methods to compute QNMs</b>	<b>24</b>
A.1	Time domain integration and Prony method	24
A.2	Direct integration	26
A.3	WKB	26

---

## 1 Introduction

Einstein’s theory has been confronted with theoretical and observational challenges that remain unresolved within its current framework. For instance, the observed flat rotation curves of galaxies [1], the accelerated expansion of the universe [2], and the problem of singularities [3]. Among these open questions, of particular importance is a complete quantum description of gravity, which is anticipated to become relevant at the Planck scale [4, 5]. Several candidates for a quantum gravity theory have been proposed to address the quantum gravity problem, including string theory [6, 7], loop quantum gravity [8, 9], causal dynamical triangulations [10], and Horava-Lifshitz gravity [11]. However, experimental verification of these theories remains a significant challenge, as direct experiments at the Planck scale are currently impractical. Nonetheless, suppressed effects originating from an underlying unified quantum gravity theory might be detectable through sensitive experiments at currently accessible low-energy scales using Effective Field Theories (EFT) [12]. Among the potential observable signatures of an underlying unified quantum gravity theory are models incorporating Lorentz symmetry breaking [13–16].

Lorentz symmetry breaking can occur either explicitly or spontaneously [17]. Explicit Lorentz symmetry breaking (ELSB) is constructed through a Lagrangian density that includes terms no longer invariant under Lorentz transformations. Alternatively, it is possible to construct a theory where Lorentz symmetry is violated in a manner that preserves the independence of physical laws from specific reference frames, ensuring that the Lagrangian remains Lorentz invariant. This occurs in the context of spontaneous Lorentz symmetry breaking (SLSB). In this framework, the trade-off is that the ground state of the physical system loses Lorentz symmetry. The core idea is that interactions

among tensor fields in the underlying theory induce the emergence of non-zero vacuum expectation values (VEVs) for Lorentz tensors. An EFT for studying SLSB is the Standard-Model Extension (SME) [17, 18]. Furthermore, SLSB is the most suitable approach for application in the gravitational sector, as it ensures the conservation of the energy-momentum tensor [19]. One of the simplest models exhibiting SLSB is the bumblebee model [17], a dynamical vectorial theory with a self-interaction potential that triggers SLSB, extensively studied in the literature [20–25]. Another candidate for SLSB is an antisymmetric rank-2 tensor field [26], also known as the Kalb-Ramond field [27], also endowed with a self-interaction potential that triggers SLSB. In both cases, if the tensor fields have non-vanishing VEVs, they define a preferred direction in the spacetime, signaling the violation of local Lorentz symmetry.

The anisotropies induced by the Lorentz-violating fields can remarkably modify the structure of compact objects, even in the absence of matter fields, as observed in Refs. [28–30] for the bumblebee model and in Refs. [31, 32] for the antisymmetric rank-2 tensor model. Nevertheless, in non-vacuum environments, these anisotropies pose significant challenges for the search for compact objects [33]. These difficulties mainly arise if the Lorentz-violating fields are solely coupled to gravity, through non-minimal couplings, where the spacetime geometry is restricted by the fields’ equations of the Lorentz-violating tensors in the VEV state. A suitable way to overcome these issues is to consider couplings between Lorentz-violating fields and matter. In this manner, the fields’ equations of the Lorentz-violating tensors are modified, allowing the emergence of novel compact objects in Lorentz-violating scenarios. Such approach was used in electro-vacuum scenarios, where spherically symmetric charged black holes could be found [34, 35]. We remark that, couplings between Lorentz-violating tensors and matter have previously been investigated in the context of metric-affine bumblebee gravity [36, 37].

Among the compact objects predicted by General Relativity (GR) and modified gravity theories, wormholes are undoubtedly considered one of the most intriguing. These ultracompact objects (UCOs), with non-trivial topology, are characterized by a minimal hypersurface—known as throat—, which serves as a bridge between two distant regions of the same or different universes. These tunnel-like structures may introduce novel features that tell wormhole apart from other UCOs. Initially, wormholes were introduced in the literature as non-traversable bridges [38, 39]. Nevertheless, in the 1970s, it was found that traversable wormholes could be supported by phantom scalar fields [40–42]. The fact that the phantom field carries the “wrong” sign in front of its kinetic term leads to the violation of some energy conditions. Although this type of matter is considered exotic, phantom fields are gaining increasing attention in cosmology in recent years, as they give rise to an accelerated expansion of the Universe, i.e., a possible explanation for dark energy [43]. Moreover, recent results from the Dark Energy Spectroscopic Instrument (DESI) combined with Type Ia supernovae (SNIa) measurements [44] may suggest a crossing of the phantom divide line. This implies that the dark energy equation-of-state parameter  $w$  crosses the cosmological constant boundary  $w_\Lambda = -1$ . Theoretically, this suggests that within the framework of GR, phantom scalar fields would be required to consistently produce a phantom equation of state  $w < -1$ .

It is widely known that wormhole solutions can emerge in Lorentz-violating frameworks. As shown in Ref. [45], it is possible to generate wormhole solutions with the VEV of a timelike antisymmetric rank-2 field by assuming an anisotropic matter source. Moreover, in Ref. [46], the counterpart of the Ellis-Bronnikov wormhole (EBWH) solution was found for the same VEV antisymmetric field non-minimally coupled to the Riemann tensor, assuming a phantom scalar field minimally coupled to gravity as matter source. This phantom field, differently from the standard EBWH, has a non-trivial self-interaction potential. Despite of this, the counterpart of the EBWH for the bumblebee gravity is still missing. In this work, we aim to derive such wormhole solution in models featuring non-

minimal couplings between the Lorentz-violating tensor fields and the Ricci tensor. We show that in order to generate such solutions, one requires the introduction of a coupling between the phantom scalar field and the Lorentz-violating fields, henceforth called LV-matter couplings, in a similar manner as introduced in Refs. [34, 35] to construct charged black hole solutions within Lorentz-violating frameworks. Under the assumption of these additional couplings, we derive EBWH analogs in three distinct Lorentz-violating scenarios: carrying contributions from the VEV of (I) the bumblebee field, (II) the antisymmetric rank-2 tensor field, and (III) a combined scenario incorporating both fields. In the latter case, despite the distinct nature of the fields, their non-zero VEV contribute additively to the overall effect on the resulting line element and on the phantom distribution that is the source of this spacetime.

We remark that the Lorentz-violating fields can also influence an independent (canonical) scalar field lying in these Lorentz-violating spacetimes. The dynamics of a test scalar field with such additional couplings could be told apart from a test scalar field minimally coupled to the spacetime metric. Thus, the investigation of scalar waves either minimally coupled to the metric or with additional LV-matter couplings is well-motivated, and an avenue for such exploration is the analysis of their distinct quasinormal mode (QNM) spectra. QNMs are characterized by complex frequencies, where the real part corresponds to the oscillation frequency and the imaginary part determines the damping rate of the oscillation. Here, we calculate the QNM spectra of canonical scalar fields coupled to Lorentz-violating fields and minimally coupled to the metric through three independent methods: direct integration, 6th-order WKB approximation, and the Prony method, finding strong agreement among the results. In particular, we find that the QNMs of scalar perturbations coupled to Lorentz-violating fields in the wormhole of case I coincide with the spectrum of scalar perturbations in the standard EBWH solution. Furthermore, we show the necessary conditions for such peculiarity happens and show that this result can be extended to black hole solutions of Einstein-bumblebee gravity [28].

The content of this paper is organized as follows. In Sec. 2, we introduce the Lorentz-violating framework we will use, and derive its field equations. The wormhole solutions supported by phantom scalar field coupled to Lorentz-violating fields are presented in Sec. 3. In Sec. 4, we investigate the dynamics of canonical scalar fields subjected either minimally coupled to the metric tensor or coupled to Lorentz-violating fields, calculating their distinct QNM spectra in Sec. 5. In Sec. 6, we examine the role of LV-matter coupling in the propagation of scalar perturbations within models featuring Lorentz symmetry breaking. Finally, we summarize our results and discuss some perspectives in Sec. 7.

## 2 Framework

Let us consider the gravity theory described by the action

$$S = \frac{1}{2\kappa} \int d^4x \sqrt{-g} (\mathcal{L}_g + \mathcal{L}_K + \mathcal{L}_V + \mathcal{L}_M), \quad (2.1)$$

where  $\mathcal{L}_g = \mathcal{L}_{EH} + \mathcal{L}_{LVg}$  is the gravitational Lagrangian, with  $\mathcal{L}_{EH} = R$  being the the Einstein-Hilbert term, where  $R$  is the Ricci tensor and  $g$  is the determinant of the metric tensor, and  $\mathcal{L}_{LVg}$  encoding the couplings of the bumblebee field,  $\mathfrak{B}_\mu$ , and the antisymmetric rank-2 tensor,  $B_{\mu\nu}$ , with curvature terms, which is given by

$$\mathcal{L}_{LVg} = \left( \tilde{\xi}_2 \mathfrak{B}^\mu \mathfrak{B}^\nu + \xi_2 B^\mu{}_\alpha B^{\alpha\nu} \right) R_{\mu\nu}. \quad (2.2)$$

The Lagrangians  $\mathcal{L}_K$  and  $\mathcal{L}_V$ , given by,

$$\mathcal{L}_K = -2\kappa \left[ \frac{1}{4} \mathfrak{B}_{\mu\nu} \mathfrak{B}^{\mu\nu} + \frac{1}{12} H_{\lambda\mu\nu} H^{\lambda\mu\nu} \right], \quad (2.3)$$

$$\mathcal{L}_V = -2\kappa \left[ \mathfrak{U}(\mathfrak{B}_\mu \mathfrak{B}^\mu \pm \mathfrak{b}^2) + V(B_{\mu\nu} B^{\mu\nu} \pm b^2) \right], \quad (2.4)$$

respectively, encode the kinetic terms of the bumblebee and the antisymmetric rank-2 tensor fields and their self-interaction potentials, while  $\mathcal{L}_M$  is the matter Lagrangian. Here,  $\mathfrak{b}$  and  $b$  are real constants, the sign in the argument of the self-interaction potentials is chosen depending on the norm of the tensor fields  $\mathfrak{B}_\mu$  and  $B_{\mu\nu}$ , specifically plus (+) if the tensor is timelike, and minus (−) if it is spacelike. Moreover,  $\mathfrak{B}_{\mu\nu}$  and  $H_{\lambda\mu\nu}$  are the field strengths of the bumblebee field and of the rank-2 antisymmetric tensor, respectively given by,

$$\mathfrak{B}_{\mu\nu} = \partial_\mu \mathfrak{B}_\nu - \partial_\nu \mathfrak{B}_\mu, \quad (2.5)$$

$$H_{\lambda\mu\nu} = \partial_\lambda B_{\mu\nu} + \partial_\mu B_{\nu\lambda} + \partial_\nu B_{\lambda\mu}. \quad (2.6)$$

We assume that the self-interaction potentials,  $\mathfrak{U}$  and  $V$ , trigger spontaneous breaking of the Lorentz symmetry. They lead to the formation of non-zero vacuum expectation value (VEV) for the bumblebee and for the 2-form field, respectively,

$$\langle \mathfrak{B}_\mu \rangle = \mathfrak{b}_\mu \quad \text{and} \quad \langle B_{\mu\nu} \rangle = b_{\mu\nu}, \quad (2.7)$$

which defines background tensor fields. Consequently, we have a local breaking of both Lorentz symmetry and diffeomorphism symmetry [19]. Within this vacuum configuration, we will explore in the subsequent sections the implications of Lorentz symmetry violation on the geometry of wormholes.

The VEV configuration is particularly interesting since it provides a simple framework for investigating the effects of LV in the gravitational sector. The potentials that drive the spontaneous breaking of Lorentz symmetry takes a simple form in this configuration. For instance, we can consider the well-known smooth quadratic potential, extensively studied in the literature [19, 47, 48], given by

$$\mathfrak{U} = \frac{1}{2} \tilde{\zeta} \mathfrak{X}^2, \quad V = \frac{1}{2} \zeta X^2 \quad (2.8)$$

where  $\tilde{\zeta}$  and  $\zeta$  are constants and  $\mathfrak{X} \equiv \mathfrak{B}_\mu \mathfrak{B}^\mu \pm \mathfrak{b}^2$  and  $X = B_{\mu\nu} B^{\mu\nu} \pm b^2$ . To ensure that (2.7) represent vacuum configurations, the constant norm conditions, expressed as

$$\mathfrak{b}^2 = \langle \mathfrak{B}_\mu \mathfrak{B}^\mu \rangle = g^{\mu\nu} \mathfrak{b}_\mu \mathfrak{b}_\nu, \quad (2.9)$$

$$b^2 = \langle B_{\mu\nu} B^{\mu\nu} \rangle = g^{\alpha\mu} g^{\beta\nu} b_{\alpha\beta} b_{\mu\nu}, \quad (2.10)$$

must be satisfied.

As discussed in Ref. [33], the assumption that the background fields couple solely to the gravity sector can impose stringent constraints on the structure of the spacetime, complicating the search for compact objects in non-vacuum environments. However, by assuming the couplings of the background fields to matter may relax the constraints on the spacetime geometry induced by the LV [34, 35]. Here, we consider possible LV-matter couplings of the background fields to a phantom scalar field, through the matter Lagrangian  $\mathcal{L}_M = \mathcal{L}_\Phi + \mathcal{L}_{LV\Phi}$ , where  $\mathcal{L}_\Phi = \kappa[\partial_\mu \Phi \partial^\mu \Phi - 2\mathcal{V}(\Phi)]$  is the standard Lagrangian of phantom scalar field with self-interaction potential  $\mathcal{V}(\Phi)$ , and

$$\mathcal{L}_{LV\Phi} = -2\kappa (\tilde{\eta} \mathfrak{B}_\mu \mathfrak{B}_\nu + \eta B_\mu{}^\alpha B_{\alpha\nu}) \partial^\mu \Phi \partial^\nu \Phi \quad (2.11)$$

encodes the LV-matter couplings, where  $\eta, \tilde{\eta}$  are coupling constants. The inclusion of these new terms not only affects the dynamics of the phantom scalar field but also modifies the gravitational dynamics. Additionally, they play a crucial role in the constraints arising from the dynamics of the background fields, as we shall see in the subsequent sections.

The gravitational field equations follow from the variation of the action (2.1) with respect to the metric, namely

$$G_{\mu\nu} = R_{\mu\nu} - \frac{1}{2}Rg_{\mu\nu} = \kappa T_{\mu\nu} \quad (2.12)$$

where  $T_{\mu\nu} = T_{\mu\nu}^{\mathfrak{B}} + T_{\mu\nu}^B + T_{\mu\nu}^\Phi + T_{\mu\nu}^{LVg} + T_{\mu\nu}^{LV\Phi}$  is the (total) energy momentum tensor, with

$$T_{\mu\nu}^{\mathfrak{B}} = -\mathfrak{B}_{\mu\alpha}\mathfrak{B}^\alpha{}_\nu - \frac{1}{4}\mathfrak{B}_{\alpha\beta}\mathfrak{B}^{\alpha\beta}g_{\mu\nu} - \mathfrak{U}g_{\mu\nu} + \mathfrak{U}_{\mathfrak{X}}\mathfrak{B}_\mu\mathfrak{B}_\nu, \quad (2.13)$$

$$T_{\mu\nu}^B = \frac{1}{2}H^{\alpha\beta}{}_\mu H_{\nu\alpha\beta} - \frac{1}{12}g_{\mu\nu}H^{\alpha\beta\lambda}H_{\alpha\beta\lambda} - g_{\mu\nu}V + 4B^\alpha{}_\mu B_{\alpha\nu}V_X,$$

$$T_{\mu\nu}^\Phi = -\frac{1}{2}\partial_\mu\Phi\partial_\nu\Phi + \frac{1}{4}\partial_\alpha\Phi\partial^\alpha\Phi g_{\mu\nu} - \frac{1}{2}\mathcal{V}(\Phi)g_{\mu\nu}, \quad (2.14)$$

$$\begin{aligned} T_{\mu\nu}^{LVg} = & \frac{\tilde{\xi}_2}{\kappa} \left( \frac{1}{2}\mathfrak{B}^\alpha\mathfrak{B}^\beta R_{\alpha\beta}g_{\mu\nu} - \mathfrak{B}^\alpha R_{\alpha\{\mu}\mathfrak{B}_{\nu\}} + \frac{1}{2}\nabla_\alpha\nabla_{\{\mu}(\mathfrak{B}_{\nu\}}\mathfrak{B}^\alpha) - \frac{1}{2}\nabla_\alpha\nabla^\alpha(\mathfrak{B}_\mu\mathfrak{B}_\nu) \right. \\ & \left. - \frac{1}{2}g_{\mu\nu}\nabla_\alpha\nabla_\beta(\mathfrak{B}^\alpha\mathfrak{B}^\beta) \right) + \frac{\xi_2}{\kappa} \left( \frac{1}{2}B^{\alpha\lambda}B^\beta{}_\lambda R_{\alpha\beta}g_{\mu\nu} - B^\alpha{}_\mu B^\beta{}_\nu R_{\alpha\beta} - B^{\alpha\beta}R_{\alpha\{\mu}B_{\nu\}\beta} \right. \\ & \left. + \frac{1}{2}\nabla_\alpha\nabla_{\{\mu}(B_{\nu\}\beta}B^{\alpha\beta}) - \frac{1}{2}\nabla_\lambda\nabla^\lambda(B^\alpha{}_\mu B_{\alpha\nu}) - \frac{1}{2}g_{\mu\nu}\nabla_\alpha\nabla_\beta(B^{\alpha\lambda}B^\beta{}_\lambda) \right) \end{aligned} \quad (2.15)$$

$$\begin{aligned} T_{\mu\nu}^{LV\Phi} = & \tilde{\eta}\mathfrak{B}^\alpha\nabla_\alpha\Phi \left( 2\mathfrak{B}_{\{\mu}\nabla_{\nu\}}\Phi - g_{\mu\nu}\mathfrak{B}_\beta\nabla^\beta\Phi \right) \\ & + \eta \left[ \left( 2B_{\mu\alpha}B_{\nu\beta} - B_{\alpha\lambda}B_{\beta\lambda}g_{\mu\nu} \right) \nabla^\alpha\Phi\nabla^\beta\Phi + 2\nabla^\alpha\Phi B_{\alpha\beta}B_{\{\nu}{}^\beta\nabla_{\mu\}}\Phi \right] \end{aligned} \quad (2.16)$$

where  $\mathfrak{U}_{\mathfrak{X}} = \partial\mathfrak{U}/\partial\mathfrak{X}$  and  $V_X = \partial V/\partial X$ .

By varying the action (2.1) with respect to  $\Phi$  one obtains the equations of motion for the scalar field, namely

$$\begin{aligned} \square\Phi + \frac{\partial\mathcal{V}}{\partial\Phi} = & 2\tilde{\eta} \left[ \mathfrak{B}^\alpha\mathfrak{B}^\beta\nabla_\alpha\nabla_\beta\Phi + \nabla_\beta\Phi\nabla_\alpha(\mathfrak{B}^\alpha\mathfrak{B}^\beta) \right] \\ & + 2\eta \left[ B_{\alpha\mu}B_{\beta\nu}\nabla^\beta\nabla^\alpha\Phi + \nabla^\alpha\Phi\nabla_\mu(B^\mu{}_\beta B_{\alpha\beta}) \right], \end{aligned} \quad (2.17)$$

where  $\square = \nabla_\alpha\nabla^\alpha$ . As we can see, the LV-matter couplings of the scalar field to the bumblebee and to antisymmetric rank-2 tensor introduce additional terms on the standard Klein-Gordon equation. The variation of the matter Lagrangian with respect to the  $\mathfrak{B}_\mu$  and  $B_{\mu\nu}$  yield, respectively, to

$$\nabla_\mu\mathfrak{B}^{\mu\nu} = 2\mathfrak{U}_{\mathfrak{X}}\mathfrak{B}^\nu - \frac{\tilde{\xi}_2}{\kappa}\mathfrak{B}^\mu R_{\mu\nu} + 2\tilde{\eta}\mathfrak{B}^\mu\nabla_\mu\Phi\nabla^\nu\Phi, \quad (2.18)$$

$$\nabla_\alpha H^{\alpha\mu\nu} = 4V_X B^{\mu\nu} + \frac{\xi_2}{\kappa}B_{\alpha}{}^{[\mu}R^{\nu]\alpha} + 2\eta B^{[\beta}{}_\mu\nabla^{\alpha]}\Phi\nabla^\mu\Phi. \quad (2.19)$$

Therefore, in order to search for wormhole solutions supported by phantom fields with LV, we must solve the metric equation (2.12) along with the dynamical equations for the phantom field (2.17) and the dynamical equations for the tensors with non-zero VEV, namely Eqs. (2.18) and (2.19). As we shall see, for suitable VEV configurations, these latter equations act as constraints on the spacetime geometry and on the scalar field profile.

### 3 Wormholes supported by phantom distributions coupled to Lorentz-violating fields

In this and in the forthcoming sections we explore the implications of allowing LV-matter distributions in the spacetime. A remarkable consequence of the inclusion of these additional terms is the possibility of simple scalar field distributions acting as sources of wormholes in Lorentz-violating backgrounds. We remark that phantom wormholes were already found in gravity frameworks considering LV-gravity couplings, for instance in Ref. [46], where these type of wormhole were found considering self-interaction phantom scalar fields in a Lorentz-violating model with the coupling of an antisymmetric rank-2 tensor with non-vanishing VEV to the Riemann tensor. Surprisingly, one of the phantom wormholes found is a simple extension of the (symmetric) Ellis-Bronnikov wormhole, namely

$$ds^2 = -dt^2 + dx^2 + \left( a^2 + \frac{x^2}{1-L} \right) (d\theta^2 + \sin^2 \theta d\varphi^2), \quad (3.1)$$

where  $L$  encodes the contributions of the VEV of the antisymmetric tensor  $B^{\mu\nu}$  and its non-minimal coupling to the Riemann tensor. As discussed in Ref. [33], phantom wormholes of this type are absent in LV backgrounds when considering non-minimal couplings to the Ricci tensor. This absence arises due to the anisotropies introduced by the non-vanishing VEV fields. However, in this work, we show that the inclusion of additional LV-matter couplings enables the emergence of such wormhole solutions in LV models with non-minimal couplings to the Ricci tensor. Furthermore, these solutions are supported by free scalar fields, providing a new perspective on the viability of phantom wormholes in LV frameworks.

Let us consider static and spherically symmetric wormholes with line element given by

$$ds^2 = -A(x)dt^2 + \frac{dx^2}{A(x)} + r(x)^2 d\Omega^2, \quad (3.2)$$

where the radial coordinate  $x \in (-\infty, \infty)$  and  $d\Omega^2 = d\theta^2 + \sin^2 \theta d\varphi^2$  is the line element of a unit sphere. Since we are looking for wormhole solutions, the areal radius  $r(x)$  is assumed to possess a minimum, that without loss of generality can be taken at  $x = 0$ , thus

$$r(0) = a, \quad r'(0) = 0, \quad r''(0) > 0 \quad (3.3)$$

where  $a$  is the radius of the wormhole throat. Moreover, the primes denotes derivatives with respect to the radial coordinate  $x$ .

Since we are adopting the line element (3.2), a stationary, spacelike VEV of the bumblebee field given by  $\mathfrak{b}_\mu = (0, b/\sqrt{A(x)}, 0, 0)$  ensures a constant norm,  $\mathfrak{b}_\mu \mathfrak{b}^\mu = \mathfrak{b}^2$ . While for the antisymmetric rank-2 tensor, as proposed in Ref. [49], it is convenient to express the VEV as  $b_{\mu\nu} = \tilde{E}_{[\mu} v_{\nu]} + \epsilon_{\mu\nu\alpha\beta} v^\alpha \tilde{B}^\beta$ , where the background vectors  $\tilde{E}_\mu$  and  $\tilde{B}_\mu$  can be interpreted as pseudo-electric and pseudo-magnetic fields, respectively, and  $v^\mu$  is a timelike 4-vector. The pseudo-fields  $\tilde{E}_\mu$  and  $\tilde{B}_\mu$  are spacelike, i.e.,  $\tilde{E}_\mu v^\mu = \tilde{B}_\mu v^\mu = 0$ . Here we consider a pseudo-electric configuration of 2-form  $\mathfrak{b}_2 = -\tilde{E}(x) dt \wedge dx$ , i.e., the only nonvanishing terms are  $b_{tx} = -b_{xt} = -\tilde{E}(x)$ , which can be determined through Eq. (2.10) for the line element (3.2), yielding a constant pseudo-electric field, expressed as  $\tilde{E} = b/\sqrt{2}$ . As a consequence, both VEV field strenghts vanish, namely  $\langle \mathfrak{B}_{\mu\nu} \rangle = 0$  and  $\langle H_{\mu\nu\alpha} \rangle = 0$ .

A direct implication of the vanishing of  $\langle \mathfrak{B}_{\mu\nu} \rangle$  and  $\langle H_{\mu\nu\alpha} \rangle$  is that the dynamical equations (2.18) and (2.19) turn into constraints on the geometry and on the matter distributions. In the VEV configuration, the anisotropies induced by the LV are encoded in the VEV equation, that for the bumblebee

and for the antisymmetric rank-2 tensor are, respectively,

$$-\frac{\tilde{\xi}_2}{\kappa} \mathfrak{b}^\mu R_{\mu}{}^\nu + 2\tilde{\eta} \mathfrak{b}^\mu \nabla_\mu \Phi \nabla^\nu \Phi = 0, \quad (3.4)$$

$$\frac{\xi_2}{\kappa} b_\alpha^{[\mu} R^{\nu]\alpha} + 2\eta b^{[\beta}{}_\mu \nabla^{\alpha]} \Phi \nabla^\mu \Phi = 0, \quad (3.5)$$

where we have used that  $\langle \mathfrak{U}_{\mathfrak{x}} \rangle = \langle V_X \rangle = 0$ , since we are considering a quadratic self-interaction potential (2.8). One notices that the LV-matter couplings between the background fields and the derivatives of the scalar field modify the constraints imposed by the VEV equations. In the absence of these additional couplings, as discussed in Ref. [33], tideless wormholes—characterized by a lapse function  $A = 1$ —, such as the one described by the line element (3.1), cannot emerge in such LV gravity frameworks. However, these wormholes can arise in LV scenarios if suitable coupling constants are considered.

To explore tideless wormholes within the gravity framework given by Eq. (2.1), we will henceforth assume  $A = 1$ . It can be observed that by substituting Eq. (3.2) into Eqs. (2.9) and (2.10) yields, respectively,

$$\mathfrak{b}_\mu = (0, \mathfrak{b}, 0, 0), \quad b_{\mu\nu} = \begin{pmatrix} 0 & -\frac{\mathfrak{b}}{\sqrt{2}} & 0 & 0 \\ \frac{\mathfrak{b}}{\sqrt{2}} & 0 & 0 & 0 \\ 0 & 0 & 0 & 0 \\ 0 & 0 & 0 & 0 \end{pmatrix}. \quad (3.6)$$

Therefore, the VEV equation of the bumblebee (3.4) and of the antisymmetric rank-2 tensor field (3.5) become, respectively,

$$\mathfrak{b} \left( \frac{\tilde{\xi}_2 r''}{\kappa r} + \tilde{\eta} \Phi'^2 \right) = 0. \quad (3.7)$$

$$b \left( \frac{\xi_2 r''}{\kappa r} + \eta \Phi'^2 \right) = 0. \quad (3.8)$$

At this stage, the necessity of introducing the LV-matter coupling becomes evident: for  $\eta = \tilde{\eta} = 0$ , Eqs. (3.7) and (3.8) are purely geometric constraints that eliminate the possibility of a local minimum in the areal function, thus ruling out the existence of a wormhole solution.

Under the VEV configuration (3.6), the gravitational field equations (2.12) reduce to the three differential equations:

$$\frac{2rr'' + r'^2 - 1}{r^2} = -\frac{1}{2}\kappa (2\tilde{\eta}\mathfrak{b}^2 + \eta b^2 - 1) \Phi'^2 + \frac{(b^2\xi_2 - 2\mathfrak{b}^2\tilde{\xi}_2) r'^2 - 4\mathfrak{b}^2\tilde{\xi}_2 rr''}{2r^2}, \quad (3.9)$$

$$\frac{r'^2 - 1}{r^2} = \frac{1}{2}\kappa (6\tilde{\eta}\mathfrak{b}^2 - 3\eta b^2 - 1) \Phi'^2 - \frac{(2\mathfrak{b}^2\tilde{\xi}_2 - b^2\xi_2) (r'^2 - 2rr'')}{2r^2}, \quad (3.10)$$

$$\frac{r''}{r} = -\frac{1}{2}\kappa (2\tilde{\eta}\mathfrak{b}^2 - \eta b^2 - 1) \Phi'^2 + \frac{r'' (b^2\xi_2 - 2\mathfrak{b}^2\tilde{\xi}_2)}{2r}, \quad (3.11)$$

while, the scalar field equation (2.17) reads

$$(-1 + 2\tilde{\eta}\mathfrak{b}^2 - \eta b^2) \left( \Phi'' + \frac{2r'\Phi'}{r} \right) = 0, \quad (3.12)$$

where we recall that we are considering a free scalar field, such that  $\partial\mathcal{V}/\partial\Phi = 0$ , and we are assuming that the scalar field inherits the symmetries of the spacetime, thus it depends solely on the radial coordinate, namely  $\Phi = \Phi(x)$ .

In the following, we will solve the system of equations (3.9-3.12) to determine the areal radius and the scalar field profile. We consider three distinct cases: modifications arising from the VEV of the bumblebee field (Case I), the rank-2 tensor field (Case II), and their combined contributions (Case III). Additionally, the resulting solutions must satisfy the constraints imposed by Eqs. (3.7) and (3.8).

### 3.1 Case I: vector (bumblebee)

First, we consider only non-trivial contributions from the non-vanishing VEV bumblebee field, i.e.,  $\mathfrak{b}^2 \neq 0$  and  $b^2 = 0$ . By subtracting Eq. (3.9) from Eq. (3.11), we obtain a differential equation solely for the areal function, namely

$$r(l_V + 1)r'' + (l_V + 1)r'^2 - 1 = 0, \quad (3.13)$$

where  $l_V = \tilde{\xi}_2 \mathfrak{b}^2$ . One can solve this differential equation imposing the existence of a minimum at  $x = 0$  according to Eq. (3.3), finding that

$$r(x) = \sqrt{a^2 + \frac{x^2}{1 + l_V}}, \quad (3.14)$$

where it follows that the Lorentz-violating parameter is constrained by  $l_V > -1$  in order to ensure the existence of a throat, since

$$r''(0) = \frac{1}{(1 + l_V)a} > 0. \quad (3.15)$$

The resulting spacetime is described by

$$ds^2 = -dt^2 + dx^2 + \left(a^2 + \frac{x^2}{1 + l_V}\right) d\Omega^2, \quad (3.16)$$

that has the same structure as Eq. (3.1) up to the sign in front of the LV parameter. In the limit  $l_V \rightarrow 0$ , the EB solution is recovered and the areal radius becomes  $r(x) = \sqrt{a^2 + x^2}$ .

By substituting the areal radius (3.14) into Eqs. (3.9) and (3.10), and then subtracting them, we find that the scalar field satisfies

$$(\Phi')^2 = \frac{2a^2(l_V + 1)(2l_V + 1)}{\kappa(1 - 4\mathfrak{b}^2\tilde{\eta})(a^2(l_V + 1) + x^2)^2}. \quad (3.17)$$

The general solution of the above differential equation reads

$$\Phi = \pm\sqrt{2} \arctan\left(\frac{x}{a\sqrt{l_V + 1}}\right) \sqrt{\frac{1 + 2l_V}{\kappa(1 - 4\mathfrak{b}^2\tilde{\eta})}} + \Phi_0, \quad (3.18)$$

where  $\Phi_0$  is an integration constant. Without loss of generality, one can take  $\Phi_0 = 0$  and choose the plus sign in the above expression. One can check that a scalar field distribution given by Eq. (3.18) satisfies the scalar field equation (3.12). It remains to verify whether the constraint introduced by the VEV equation (3.7) is satisfied. By substituting Eqs. (3.14) and (3.18) into Eq. (3.7), one notices that the constraint is satisfied only if

$$\tilde{\eta} = -\frac{\tilde{\xi}_2}{2}, \quad (3.19)$$

that is, it is required a specific relation between the LV-matter coupling constant,  $\tilde{\eta}$ , and the LV-gravity coupling constant,  $\tilde{\xi}_2$ . A similar relation is found in Ref. [34] for LV-matter couplings of electromagnetic fields and non-vanishing VEV fields. Substituting the relation (3.19) into the expression for the scalar field (3.18), we find that the source of the wormhole (3.16) is the scalar field distribution

$$\Phi = \sqrt{2/\kappa} \arctan\left(\frac{x/a}{\sqrt{1+l_V}}\right). \quad (3.20)$$

We notice that in the limit  $l_V \rightarrow 0$ , the scalar field of EB solution is recovered.

Therefore, we present the first EB-like wormhole sourced by a free scalar field in the bumblebee gravity framework. The shape of the wormhole is changed by the anisotropy induced by the spacelike VEV of the bumblebee field supported by phantom field subject to LV-matter couplings.

### 3.2 Case II: antisymmetric rank-2 tensor

Now, we consider only non-trivial contributions from the non-vanishing VEV antisymmetric field, i.e., assuming  $b^2 \neq 0$  and  $\mathfrak{b}^2 = 0$ . Note that when we subtract Eq. (3.9) from Eq. (3.11), we find that

$$r(l_T + 1)r'' - (l_T - 1)r'^2 - 1 = -b^2\eta\kappa r^2\Phi'^2, \quad (3.21)$$

where  $l_T = \xi_2 b^2/2$ . Thus, we obtain a differential equation that depends not only on the areal radius but also on the scalar field, unlike the case with the VEV bumblebee field (3.13). Therefore, for this type of VEV configuration, there are certain subtleties and the derivation of wormhole solutions is not that direct. We can subtract Eq. (3.9) from Eq. (3.10) in order to obtain a relation between the first derivative of the scalar field and the areal radius. By doing so, we get the following expression

$$\Phi'^2 = \frac{2(1-l_T)r''}{(b^2\eta+1)\kappa r}. \quad (3.22)$$

Before substituting the above relation into Eq. (3.21) to derive an equation for the areal radius only, we can ensure that the constraint (3.8) is satisfied. This is achieved by substituting Eq. (3.22) into Eq. (3.21). It is straightforward to verify that, similarly as the case I, the constraint is satisfied only if

$$\eta = -\frac{\xi_2}{2}. \quad (3.23)$$

Thus, again it is required a specific relation between the LV-matter coupling constant,  $\eta$ , and the LV-gravity coupling constant,  $\xi_2$ .

Substituting Eq. (3.22) into Eq. (3.21) together with the relation (3.23), we obtain an equation solely for the areal function, namely

$$-r(l_T - 1)r'' - (l_T - 1)(r')^2 - 1 = 0. \quad (3.24)$$

The solution of the above equation, assuming a throat at  $x = 0$  (3.3), is given by

$$r(x) = \sqrt{a^2 + \frac{x^2}{1-l_T}}. \quad (3.25)$$

Note that, since  $r''(0) = 1/a(1-l_T)$ , the throat structure is guaranteed only if  $l_T < 1$ . The resulting spacetime is described by

$$ds^2 = -dt^2 + dx^2 + \left(a^2 + \frac{x^2}{1-l_T}\right) d\Omega^2, \quad (3.26)$$

that has the very same structure as Eq. (3.1). In the limit  $l_T \rightarrow 0$ , the EB solution is recovered.

The scalar field distribution that is the source of the wormhole (3.26) is found by substituting the areal radius (3.25) into Eq. (3.22) and integrating the resulting equation, where one obtains

$$\Phi = \sqrt{2/\kappa} \arctan\left(\frac{x/a}{\sqrt{1-l_T}}\right), \quad (3.27)$$

where we have chosen, without loss of generality, the solution with plus sign and with vanishing integration constant and additionally have set  $\eta = -\xi_2/2$  in order to verify the VEV constraint.

Therefore, we show that EB-like wormholes can arise in LV frameworks considering non-minimal couplings of non-vanishing VEV antisymmetric rank-2 tensor to Ricci tensor, and not only in frameworks considering the non-minimal coupling to the Riemann tensor. Here, nevertheless, the scalar field that supports it does not have a self-interaction potential.

### 3.3 Case III: vector and antisymmetric rank-2 tensor

Finally, let us consider the contributions from both bumblebee and antisymmetric field with non-vanishing VEV, i.e., assuming simultaneously  $b^2 \neq 0$  and  $\tilde{b}^2 \neq 0$ . In this scenario, we adopt the same approach used in the case of the antisymmetric field. Specifically, by subtracting Eqs. (3.9) and (3.10), we obtain an expression for the derivative of the scalar field with respect to the areal function, given by:

$$\Phi'^2 = \frac{2(l_T - 2l_V - 1)r''}{(4\tilde{b}^2\tilde{\eta} - b^2\eta - 1)\kappa r}. \quad (3.28)$$

Substituting the above equation into the VEV constraints (3.7) and (3.8), we obtain the following algebraic equations

$$2(l_T - 1)\tilde{\eta} - \frac{2l_T\tilde{\xi}_2}{\xi_2}\eta - \tilde{\xi}_2 = 0. \quad (3.29)$$

$$\frac{4l_V\xi_2}{\tilde{\xi}_2}\tilde{\eta} - 2(2l_V + 1)\eta - \xi_2 = 0, \quad (3.30)$$

Thus, it is straightforward to verify that the relations (3.19) and (3.23) are the only solutions of the above system.

To obtain the areal radius, we can subtract Eq. (3.9) from Eq. (3.11), and then substitute Eq. (3.28). By applying the relations (3.19) and (3.23), we find a differential equation solely for the areal radius, namely

$$r(-l_T + l_V + 1)r'' + (-l_T + l_V + 1)r'^2 - 1 = 0. \quad (3.31)$$

By imposing that there is a throat structure at  $x = 0$ , we obtain

$$r(x) = \sqrt{a^2 + \frac{x^2}{1 + l_V - l_T}}, \quad (3.32)$$

that is the areal radius that incorporates both the effects of LV from the VEV of the bumblebee and from the VEV of the antisymmetric tensor field. We remark that, a throat is present only if  $l_V - l_T > -1$ .

The phantom field that supports such structure is obtained by substituting the areal radius (3.32) into (3.28), with (3.19) and (3.23), and integrating the resulting equation, where we find that

$$\Phi = \sqrt{2/\kappa} \arctan\left(\frac{x/a}{\sqrt{1+l_V-l_T}}\right), \quad (3.33)$$

where we have chosen, without loss of generality, the solution with plus sign and with vanishing integration constant.

The resulting spacetime is described by

$$ds^2 = -dt^2 + dx^2 + \left( a^2 + \frac{x^2}{1 + l_V - l_T} \right) d\Omega^2, \quad (3.34)$$

that corresponds to an EB-like wormhole, which is supported by a phantom scalar field coupled to both the bumblebee field and the antisymmetric tensor field, each possessing a non-zero VEV. If simultaneously  $l_V \rightarrow 0$  and  $l_T \rightarrow 0$ , we recover the EB wormhole solution. Notably, if the LV parameters satisfy  $l_V = l_T$ , the line element in Eq. (3.34) also simplifies to that of the EB wormhole. This result puts light in the importance of verifying whether more astrophysically relevant solutions, such as black holes, can incorporate distinct combinations of LV parameters, since it indicates that experiments focusing solely on quantities minimally coupled to the spacetime metric might hide signatures of LV if different Lorentz-violating fields are considered.

### The structure of Lorentz-violating wormholes

Before we end this section, let us discuss some distinct characteristics that LVWHs have compared to standards EBWHs. Notably, the three wormholes reported here have the same qualitative structure as wormhole (3.1). Several notable properties of this spacetime have been investigated in Ref. [46]. For instance, far from the throat these wormholes does not approach a flat region, rather their equatorial plane display a conical geometry with a deficit (or excess) angle  $\delta$ . Specifically for the wormhole of case III it reads  $\delta = \pi(l_T - l_V)/(l_T - l_V - 1)$ . Such structure can be visualized in Fig. 1, where we exhibit the embedding diagrams of the equatorial plane of EB wormholes and of LVWH of case I with  $l_V = 0.5$ . Due to this conical behavior, the geodesic structure of the LVWHs is clearly told apart from the one of EB wormholes. As a consequence, the lensing properties of these wormholes change compared to EB wormholes, even in the weak-field approximation, where one finds that the total deflection angle of massless particles bears deviations induced by the LV. Concerning wormholes of the case III, configurations with  $l_V = l_T$  do not exhibit any angle defect, i.e.,  $\delta = 0$ , once the EB geometry is restored.

It is worth mentioning that, similar to EB wormholes, these tideless wormholes possess a single light ring located at their throats. The (in)stability of these light rings can be computed through the principal Lyapunov exponents. Specifically for tideless wormholes of case III, the principal Lyapunov exponent for massless particles in circular motion at the throat reads [50]

$$\lambda = \sqrt{\frac{r''(0)}{r(0)}} = \frac{1}{a\sqrt{1 + l_V - l_T}}. \quad (3.35)$$

Thus, the light rings at the throat correspond to unstable circular orbits, where we recall that in order to a throat-like structure to be present  $1 + l_V - l_T > 0$ . Notably, the instability of circular motion at the throat is influenced by the LV. We remark that light rings at the throats of configurations with  $l_V = l_T$  share the same Lyapunov exponents as the ones in EB wormholes.

## 4 Dynamics of scalar perturbations in Lorentz-violating wormholes

The study of how the LVWH models, introduced in the previous section, respond to perturbations provides critical insights into how the breaking of Lorentz symmetry affects the structure and stability of wormholes. To gain valuable intuition into these effects, in this and the following sections, we will

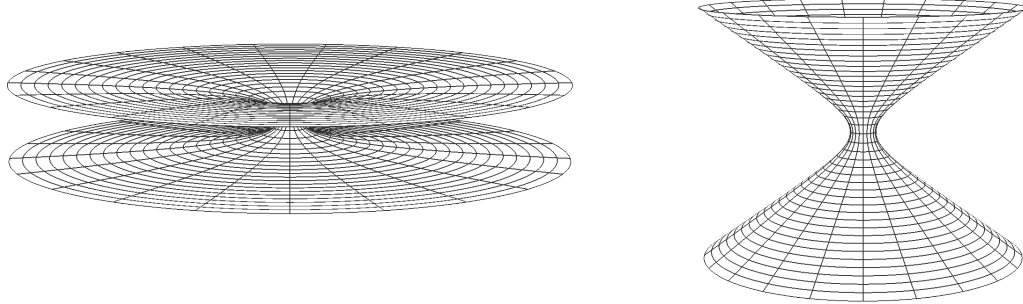


**Figure 1.** Embedding diagrams of the equatorial plane of EB wormhole (left) and LVWH of case I (right) with  $l_V = 0.5$ .

analyze the response of the LVWH models to a massless (canonical) test scalar field, denoted by  $\Psi$ . This serves as the simplest wave-like probe that can be introduced into the geometry. It is important to note that the scalar field  $\Psi$  is distinct from the phantom scalar field  $\Phi$ , which is responsible for generating the wormhole geometry. Furthermore, we assume that the scalar field  $\Psi$  does not backreact on the underlying spacetime.

The dynamics of a canonical test scalar field in a LVWH background depends critically on whether the field is assumed to solely minimally couple to the metric tensor or if it also couples with the Lorentz-violating fields. This distinction plays a crucial role in determining the behavior and evolution of the scalar field within the LVWH framework. Let us consider both scenarios and highlight their differences. In order to facilitate the study, let us split the analysis and denote  $\Psi_g$  a canonical scalar field minimally coupled to the spacetime metric and  $\Psi_{LV}$  a canonical scalar field coupled to the spacetime metric and to Lorentz-violating fields.

Hence, the dynamics of  $\Psi_g$  is described by the standard Klein-Gordon equation, namely

$$\square\Psi_g = 0, \quad (4.1)$$

while the dynamics of  $\Psi_{LV}$  is described by, cf. Eq. (2.17),

$$\nabla_\mu(q^{\mu\nu}\nabla_\nu\Psi_{LV}) = 0, \quad (4.2)$$

where, under the VEV configurations considered here,  $q^{\mu\nu} := g^{\mu\nu} + 2\tilde{\eta}b^\mu b^\nu + 2\eta b^{\mu\alpha}b^\nu{}_\alpha$  and we have used the metric compatibility condition. Let us consider that the scalar perturbations can be

decomposed using the spherical harmonics,  $Y_{\ell m}(\theta, \varphi)$ , namely

$$\Psi_g = \sum_{\ell, m} \int d\omega \frac{\psi_g(x)}{r(x)} e^{-i\omega t} Y_{\ell m}(\theta, \varphi), \quad (4.3)$$

$$\Psi_{LV} = \sum_{\ell, m} \int d\omega \frac{\psi_{LV}(x)}{r(x)} e^{-i\omega t} Y_{\ell m}(\theta, \varphi), \quad (4.4)$$

where  $Y_{\ell m}(\theta, \varphi) = P_\ell(\cos \theta) e^{im\varphi}$ , with  $P_\ell(\cos \theta)$  being the Legendre polynomials,  $\omega$  is the frequency,  $\ell$  and  $m$  are, respectively, the polar and azimuthal indices and  $\psi_g(x)$  and  $\psi_{LV}(x)$  are the radial parts of the perturbations  $\Psi_g$  and  $\Psi_{LV}$ , respectively. Due to the spherical symmetry, henceforth,  $m$  is set to zero. By plugging the scalar field decompositions into the scalar field equations (4.1) and (4.2), one obtains that the radial part of the scalar perturbations  $\Psi_g$  and  $\Psi_{LV}$  are determined, respectively, by the Schrödinger-like equations

$$\psi_g'' = U_{\omega\ell}^g(x) \psi_g, \quad (4.5)$$

$$\psi_{LV}'' = U_{\omega\ell}^{LV}(x) \psi_{LV} \quad (4.6)$$

where  $U_{\omega\ell}^g(x)$  and  $U_{\omega\ell}^{LV}(x)$  are the effective potentials the scalar perturbations  $\Psi_g$  and  $\Psi_{LV}$  are subjected, respectively. Let us explicitly show Eqs. (4.5) and (4.6) for the three above discussed LVWH cases.

### Case I

Particularly, for LVWHs of case I ( $l_V \neq 0$  and  $l_T = 0$ ), the radial part of the scalar perturbations  $\Psi_g$  and  $\Psi_{LV}$  obey, respectively,

$$\psi_g'' + \left[ \omega^2 - \frac{(1+l_V)(1+\ell(\ell+1)(1+l_V))a^2 + \ell(\ell+1)x^2}{(a^2(1+l_V) + x^2)^2} \right] \psi_g(x) = 0, \quad (4.7)$$

$$\psi_{LV}'' + \left[ \frac{\omega^2}{1+l_V} + \frac{a^2(l_V+1)(\ell^2 + \ell + 1) - \ell(\ell+1)x^2}{(a^2(l_V+1) + x^2)^2} \right] \psi_{LV}(x). \quad (4.8)$$

Surprisingly, it follows that, by introducing a re-scaled radius  $\rho = x/\sqrt{1+l_V}$ , the radial part of the scalar perturbation  $\Psi_{LV}$  obeys

$$\frac{d^2\psi_{LV}}{d\rho^2} + \left[ \omega^2 - \frac{(1+\ell(\ell+1))a^2 + \ell(\ell+1)\rho^2}{(a^2 + \rho^2)^2} \right] \psi_{LV}(\rho) = 0. \quad (4.9)$$

Remarkably, this is the same equation that the radial part of scalar perturbations obeys in the background of symmetric (massless) EB wormholes in the absence of any trait of LV [51]. At first glance, this result may appear counterintuitive, as it suggests that the scalar field perturbation is unaffected by the LV. However, as we shall see, such peculiarity follows from the couplings of the bumblebee field to derivatives of the scalar field. In Sec. 6 we provide the necessary conditions for the perturbations scalar fields subjected to the LV-matter couplings propagate in LV backgrounds as they were propagating in standard GR background (without any trait of LV). Conversely it is not possible under a change of coordinates to turn the equation of the radial part of  $\Psi_g$  into Eq. (4.9). Hence, a test scalar field minimally coupled to the metric of the LVWH of case I has its dynamics directly influenced by the LV parameter  $l_V$ .

## Case II

On the other hand, for LVWHs of case II ( $l_T \neq 0$  and  $l_V = 0$ ), the dynamics of the scalar field perturbations obey, respectively

$$\psi_g'' + \left[ \omega^2 - \frac{(1-l_T)(1+\ell(\ell+1)(1-l_T))a^2 + \ell(\ell+1)x^2}{(a^2(1-l_T) + x^2)^2} \right] \psi_g(x) = 0, \quad (4.10)$$

$$\psi_{LV}'' + \left[ \omega^2 + \frac{a^2(l_T-1)(\ell^2 + \ell + 1) - \ell(\ell+1)x^2}{(x^2 - a^2(l_T-1))^2} \right] \psi_{LV}(x). \quad (4.11)$$

Hence, as one can verify, it is not possible to transform the above equations for the radial parts of  $\Psi_g$  and  $\Psi_{LV}$  into Eq. (4.9). Therefore, differently from the bumblebee case, the dynamics of test scalar fields are directly influenced by the LV parameter regardless the LV-matter couplings.

## Case III

Finally, the case III, where both  $\mathfrak{b}$  and  $b$  are non-vanishing, is remarkably interesting. In this case, the scalar perturbations satisfy, respectively,

$$\psi_g'' + \left[ \omega^2 - \frac{(1+l_V-l_T)(1+\ell(\ell+1)(1+l_V-l_T))a^2 + \ell(\ell+1)x^2}{(a^2(1+l_V-l_T) + x^2)^2} \right] \psi_g(x) = 0, \quad (4.12)$$

$$\psi_{LV}'' + \left[ \frac{(1-l_T)\omega^2}{1+l_V-l_T} - \frac{-a^2(l_T-l_V-1)(\ell^2 + \ell + 1) + \ell(\ell+1)x^2}{(x^2 - a^2(l_T-l_V-1))^2} \right] \psi_{LV}(x) = 0. \quad (4.13)$$

By introducing a re-scaled radius  $\varrho = x\sqrt{(1+l_V-l_T)/((1-l_T))}$ , the equation for  $\psi_{LV}$  becomes

$$\frac{d^2\phi}{d\varrho^2} + \left[ \omega^2 - \frac{-a^2(l_T-1)(\ell^2 + \ell + 1) + \ell(\ell+1)\varrho^2}{(\varrho^2 - a^2(l_T-1))^2} \right] \phi(\varrho) = 0, \quad (4.14)$$

and one notices that, it acquires the same form as Eq. (4.11), and therefore the contribution of  $l_V$  on the equation of the radial part of the perturbation is absent, similarly to what happens in the case I. On the other hand, the equation for  $\psi_g$  cannot be cast without the dependence on the bumblebee parameter  $l_V$ . Thus, under the VEV configuration considered here, the minimally coupled test scalar field depends on both LV parameters. Remarkably, if  $l_V = l_T$ , the dynamics of  $\psi_g$  is the same as the dynamics of a scalar field perturbation in massless Ellis-Bronnikov wormhole.

### 4.1 Effective potential

Part of understanding the behavior of perturbations in the vicinity of compact objects relies on understanding the behavior of the effective potential the perturbation is subjected. As we have seen, if the scalar perturbation under study is assumed to be solely minimally coupled to the metric, the contributions of the spacelike VEV configuration  $\mathfrak{b}^\mu$  and on the timelike VEV configuration  $b^{\mu\nu}$  are explicit on the effective potential. However, if the scalar perturbation under study is assumed to be subjected to additional LV-matter couplings, the contributions of the spacelike VEV configuration  $\mathfrak{b}^\mu$  is suppressed by a re-scale of the radial coordinate. Conversely, the same is not true for the timelike VEV configuration  $b^{\mu\nu}$ , where no re-scale of the radial coordinate remove the contribution of  $l_T$  from the radial part of the perturbation.

First, let us analyze the behavior of  $U_{\omega\ell}^g$ , the effective potential that  $\Psi_g$  is subjected, for the LVWH models. By analyzing the three cases, one notices that the effective potentials of Cases I and

II can be recovered from Case III by taking  $l_V \rightarrow 0$  and  $l_T \rightarrow 0$ , respectively. Thus, it suffices to investigate the behavior of the effective potential for the Case III, that is given by

$$U_{\omega\ell}^g = -\omega^2 + \frac{(1+l_V-l_T)(1+\ell(\ell+1)(1+l_V-l_T))a^2 + \ell(\ell+1)x^2}{(a^2(1+l_V-l_T) + x^2)^2}. \quad (4.15)$$

Interestingly, if  $l_V = l_T$  the effective potential becomes the one of scalar perturbations in EBWHs, regardless the absolute values of the LV parameters. One can check that, the asymptotic behavior of the effective potential is

$$\lim_{x \rightarrow \pm\infty} U_{\omega\ell}^g = -\omega^2, \quad (4.16)$$

that is, it goes to a negative constant values at both infinities regardless the value of  $l_V$  and  $l_T$ . One can check that for  $l_T - l_V < 1/2$ , regardless the value of  $\ell$ , the effective potential has only one critical point located at the throat. For  $\ell \neq 0$ , the effective potential can present more than one critical point. Specifically, if  $\ell = 1$ , the effective potential has three critical points if  $l_T - l_V = 1$ , and if  $\ell \geq 2$ , the effective potential has three critical points if  $1/2 + 1/\ell(\ell+1) < l_T - l_V \leq 1$ . Since we are considering solely small deviations introduced from the LV, the typical profile of the effective potential shall exhibit only one critical point, specifically a maximum. We show in the left panel of Fig. 2 the radial dependence of the effective potential, that is  $U_{\omega\ell}^g + \omega^2$ . As we can see, as  $l_V - l_T$  diminishes, the peak of the effective potential gets higher.

Regarding  $U_{\omega\ell}^{LV}$ , since the contributions of the spacelike VEV configuration  $b^\mu$  is suppressed by a re-scale of the radial coordinate, it suffices to investigate the behavior of the effective potential for the case II, given by

$$U_{\omega\ell}^{LV} = -\omega^2 + \frac{-a^2(l_T - 1)(\ell^2 + \ell + 1) + \ell(\ell + 1)x^2}{(x^2 - a^2(l_T - 1))^2}. \quad (4.17)$$

One notices that the dependence of the effective potential on the frequency decouples from the dependence on the radial coordinate. One can check that, the asymptotic behavior of the effective potential is

$$\lim_{x \rightarrow \pm\infty} U_{\omega\ell}^{LV} = -\omega^2, \quad (4.18)$$

hence, it goes to a negative constant values at both infinities. Additionally, for  $l_T < 1$ , the effective potential has a single peak located at  $x = 0$ . In the right panel of Fig. 2 we plot the profile of the part of the effective potential that does not depend on  $\omega$ , that is  $U_{\omega\ell}^{LV} + \omega^2$ . As we can see, as  $l_T$  increases, the peak of the effective potential gets higher.

## 5 Quasinormal frequencies

QNMs represent the characteristic oscillations of a perturbed physical system. In the context of wormholes, the boundary conditions imposed on the perturbations require purely outgoing waves at both spatial infinities, expressed as

$$\lim_{x \rightarrow \pm\infty} \psi \sim \exp(\pm i\omega x). \quad (5.1)$$

Each mode is characterized by a complex frequency,  $\omega$ , where the real part,  $\text{Re}[\omega]$ , corresponds to the standard oscillation frequency, and the imaginary part,  $\text{Im}[\omega]$ , determines the rate of damping or amplification of the wave. Specifically, a negative  $\text{Im}[\omega]$  indicates damping, while a positive  $\text{Im}[\omega]$  signifies amplification. These modes play a crucial role in analyzing the ringdown phase following

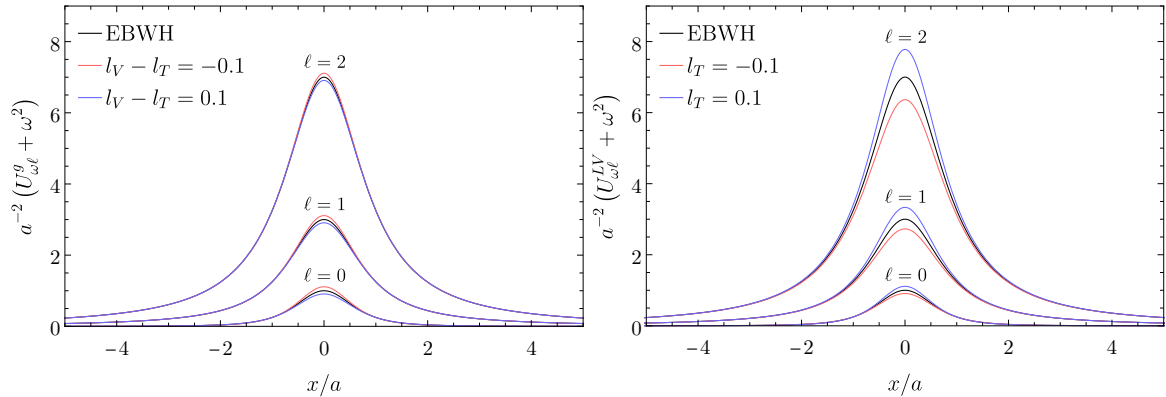


**Figure 2.** Caption

the coalescence of compact objects [52, 53], such as black holes or neutron stars. Additionally, QNMs provide valuable insights into the stability (or instability) of such compact objects [54], making them a key tool in gravitational wave astronomy and theoretical physics.

The study of the QNMs of EBWHs was extensively performed in the literature [54–57]. In this section, we provide the analysis of the quasinormal frequencies associated to test scalar fields lying in the LVWH backgrounds. As we have seen, the assumption of the LV-matter coupling provides non-trivial contributions on the scalar dynamics, thus it is expected that the QNM profile of the scalar perturbations  $\Psi_g$  and  $\Psi_{LV}$  are different.

## Results

Here we present a selection of our numerical results for the spectrum of QNMs of scalar field perturbations within a Lorentz-violating background. These results were obtained using the methods discussed in the Appendix A, considering both scalar perturbations minimally coupled to the geometry and scalar perturbations with additional LV-matter couplings. Here we will focus on the fundamental modes, with  $n = 0$ .

First, let us consider the results for the scalar perturbation  $\Psi_g$ . In Fig. (3) we show the real (left panel) and the imaginary (right panel) parts of the QNM frequencies, computed using DI, of scalar perturbations minimally coupled to gravity within LVWH of Case III. In this scenario, the value of  $\text{Re}[\omega]$  decreases as the difference between LV parameters  $l_V - l_T$  increases. Conversely,  $\text{Im}[\omega]$  increases as  $l_V - l_T$  increases, indicating that the modes are less damped as we increase the LV parameter. We notice that the QNMs of these scalar fields in LVWH are always damped, corresponding to stable perturbations.

In Fig. 4 we show the time-domain profiles of the scalar field perturbation minimally coupled to gravity within the LVWH of Case III for three polar indices, specifically  $\ell = 0, 1$  and  $2$ , and two values of difference between LV parameters, namely  $l_V - l_T = 0.1$  and  $-0.1$ . In each panel of the figure we compare the time-domain profile of the scalar perturbation in LVWH with the one of scalar perturbations in EBWH (or similarly if  $l_V = l_T$ ). We can clearly see the three stages discussed in the above section. For intermediate times, where the QNMs dominate, we can indeed see that the perturbations are more damped for smaller values of the difference  $l_V - l_T$  compared to the EBWH. After the ringdown time, one appreciates the typical tail stage, with power-law decay that seems to be independent of the LV.

We extract the QNM frequencies of the fundamental mode from the intermediate times using the Prony method and exhibit it, together with the QNM frequencies computed via DI and 6th-order

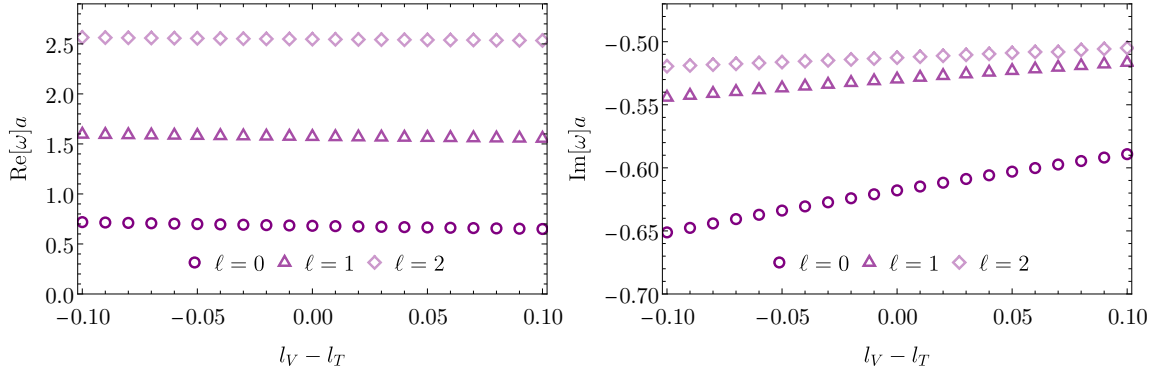


**Figure 3.** Real (left panel) and imaginary (right panel) parts of the QNMs of scalar fields minimally coupled to gravity in LVWHs of case III.

WKB in Table 1. As we can see, we find excellent agreement between the three methods.

**Table 1.** Quasinormal frequencies computed via DI, 6th-order WKB and Prony methods.

$\ell$	$l_V - l_T$	Method	$\text{Re}[\omega]a$	$-\text{Im}[\omega]a$
0	-0.1	DI	0.718331	0.651175
		WKB	0.691529	0.704740
		Prony	0.718678	0.651793
	0	DI	0.681431	0.617870
		WKB	0.656042	0.668575
		Prony	0.681298	0.617775
	0.1	DI	0.649596	0.589163
		WKB	0.625512	0.637461
		Prony	0.650444	0.589188
1	-0.1	DI	1.595446	0.544144
		WKB	1.602689	0.546061
		Prony	1.595667	0.543993
	0	DI	1.572708	0.529700
		WKB	1.576355	0.533059
		Prony	1.572913	0.529558
	0.1	DI	1.554710	0.516504
		WKB	1.556085	0.520063
		Prony	1.554904	0.516367
2	-0.1	DI	2.564324	0.519491
		WKB	2.567154	0.515875
		Prony	2.564896	0.519174
	0	DI	2.546656	0.512668
		WKB	2.548319	0.511121
		Prony	2.547213	0.512359
	0.1	DI	2.533540	0.504946
		WKB	2.534318	0.504411
		Prony	2.534084	0.504644

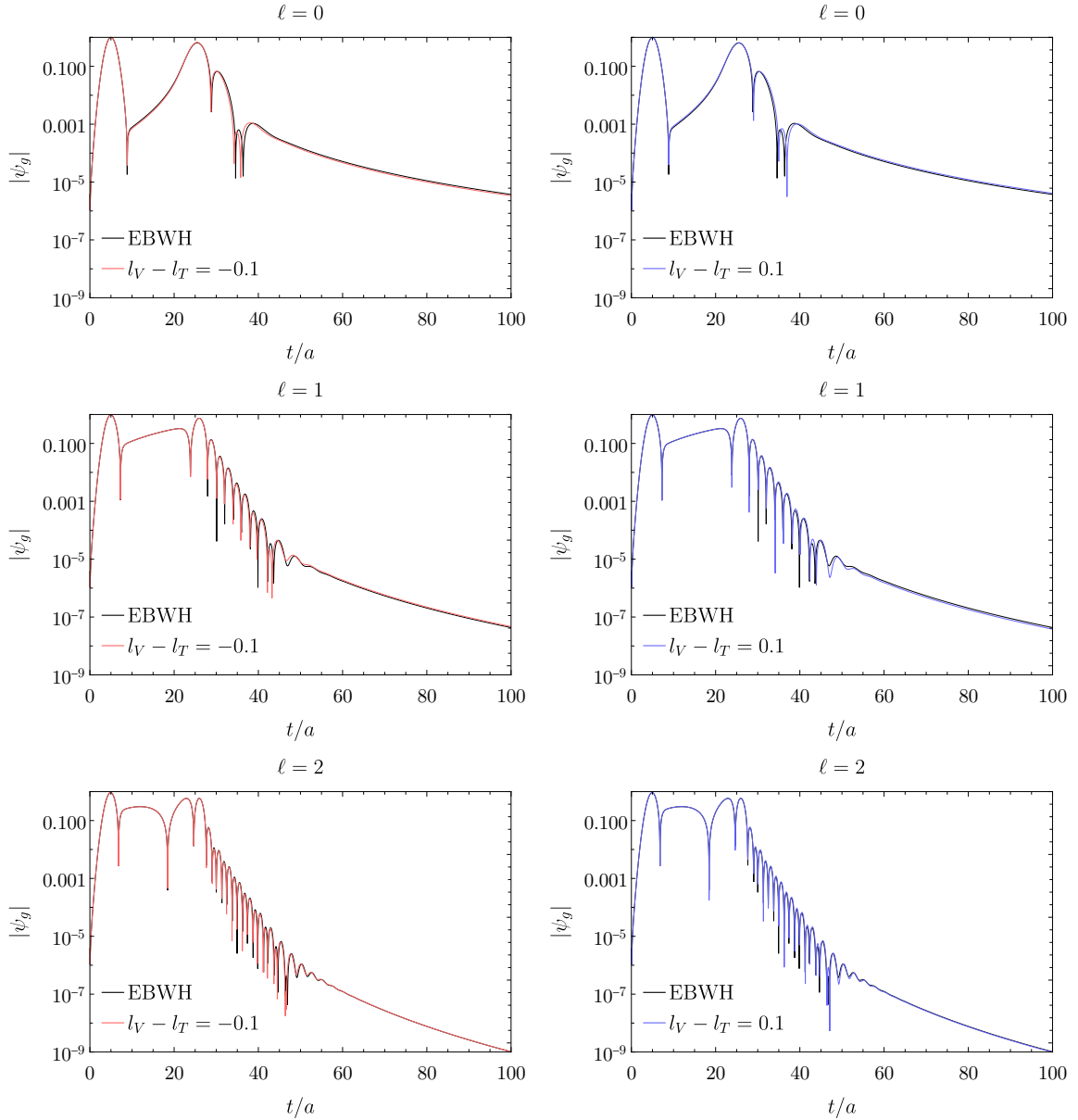


**Figure 4.** Temporal evolution data of phatom perturbations in LVWHs. The black lines correspond to the perturbation of a phatom scalar field in EBWH in the absence of LV.

Now, let us consider the results for the scalar perturbation  $\Psi_{LV}$ . In Fig. (5) we show the real (left panel) and the imaginary (right panel) parts of the QNM frequencies, computed using DI, of scalar perturbations subjected to LV-matter couplings lying in the LVWH spacetime. In this scenario, the value of  $\text{Re}[\omega]$  increases as the LV parameter  $l_T$  increases. Conversely,  $\text{Im}[\omega]$  decreases as the LV parameter  $l_T$  increases, indicating that the modes are more damped as we increase the LV parameter. We notice that, similarly to the EBWH case, the QNMs of the scalar field  $\Psi_{LV}$  are always damped, thus corresponding to stable perturbations.

In Fig. 6 we depict the time-domain profiles of the scalar field perturbation subjected to LV-matter couplings in the LVWH of Case II for three polar indices, specifically  $\ell = 0, 1$  and 2, and two

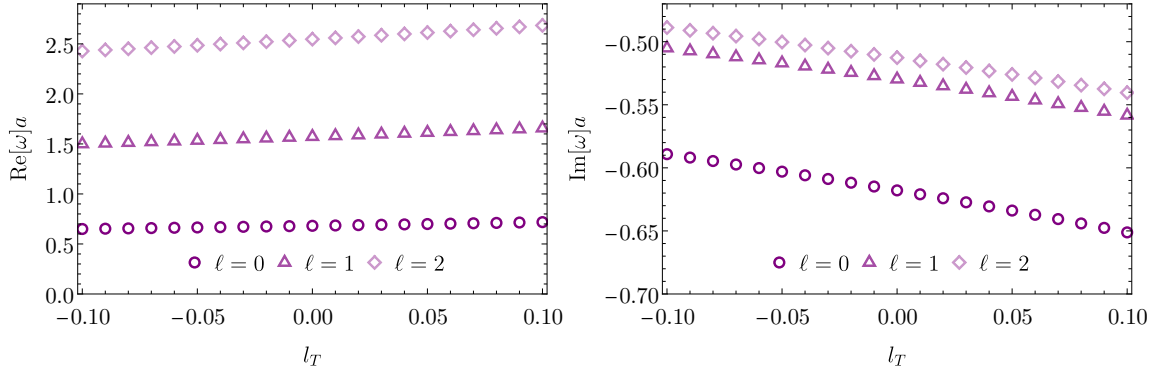


**Figure 5.** Real (left panel) and imaginary (right panel) parts of the QNMs of phantom scalar fields subjects to LV-matter couplings in LVWHs of case II.

values of LV parameter, namely  $l_T = 0.1$  and  $-0.1$ . In each panel of the figure we compare the time-domain profile of the scalar perturbation in LVWH with the one of scalar perturbations in EBWH. We can clearly see the three stages discussed in the above section. We can see that the perturbations are less damped for smaller values of LV parameter compared to the EBWH. After the ringdown time, the power-law tail stage seems to be independent of the LV.

We extract the QNM frequencies of the fundamental mode from the intermediate times using the Prony method and exhibit it, together with the QNM frequencies computed via DI and 6th-order WKB in Table 2. As we can see, we find excellent agreement between the three methods.

## 6 A note on scalar perturbations subjected to couplings to Lorentz-violating fields

The intriguing fact of the scalar perturbation  $\Psi_{LV}$  does not present LV factors on its dynamics in the LVWH of case I is a consequence of the LV-matter coupling. However, one would ask if this counterintuitive behavior is also directly related to the fact that the VEV configuration  $\mathfrak{b}^\mu$  is a constant spacelike field. Let us illustrate that the same intriguing behavior happens even for non-constant spacelike VEV configurations, such as the ones considered in vacuum spherically symmetric bumblebee black holes [28], and use it as a guideline to deduce the necessary conditions for such behavior to happen.

First, let us consider a spherically symmetric solution of the gravity framework

$$S = \frac{1}{2\kappa} \int d^4x \sqrt{-g} \left( R + \tilde{\xi}_2 \mathfrak{B}^\mu \mathfrak{B}^\nu R_{\mu\nu} - \frac{\kappa}{2} \mathfrak{B}_{\mu\nu} \mathfrak{B}^{\mu\nu} - 2\kappa \mathfrak{U}(\mathfrak{X}) \right), \quad (6.1)$$

given by

$$ds^2 = - \left( 1 - \frac{2M}{r} \right) dt^2 + \frac{1 + l_V}{1 - \frac{2M}{r}} dr^2 + r^2 d\Omega^2, \quad (6.2)$$

with VEV configuration  $\mathfrak{b}_\mu = (0, \mathfrak{b} \sqrt{1 + l_V} / \sqrt{1 - 2M/r}, 0, 0)$  triggered by the self-interaction term  $\mathfrak{U}(\mathfrak{X}) = \frac{1}{2} \tilde{\zeta} (\mathfrak{B}^\mu \mathfrak{B}^\nu - \mathfrak{b}^2)^2$ , such that  $\mathfrak{b}_\mu \mathfrak{b}^\mu = \mathfrak{b}^2$  is constant. Here,  $M$  stands for the mass of the black hole and  $l_V$  has the same definition of the previous sections, namely  $l_V = \tilde{\xi}_2 \mathfrak{b}^2$ .

Now, let us additionally assume that there is a test scalar field subjected to a LV-matter coupling lying in this spherically symmetric spacetime, such that its dynamics is described by

$$\nabla_\mu (h^{\mu\nu} \nabla_\nu \Psi) = 0, \quad (6.3)$$

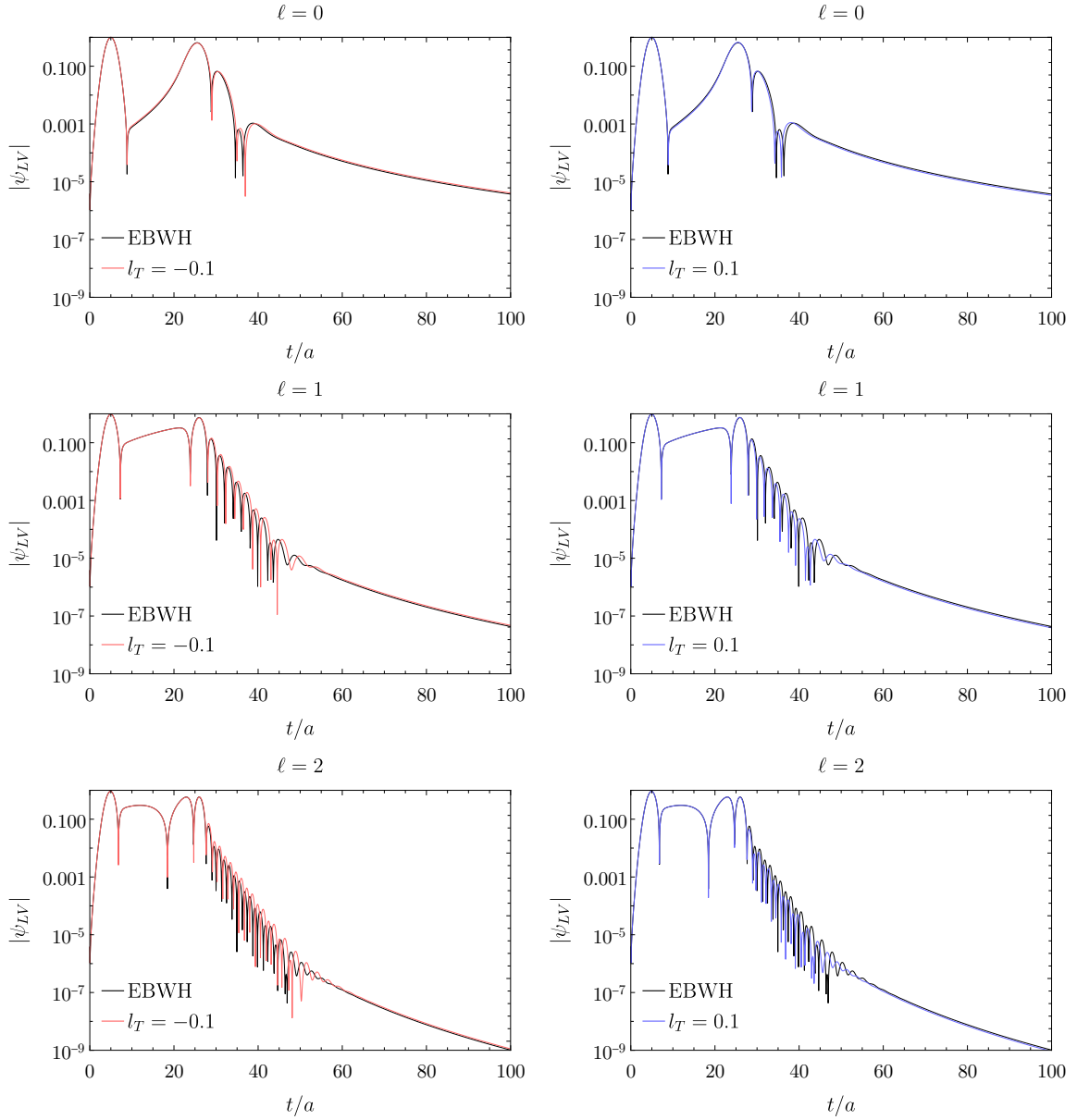


**Figure 6.** Temporal evolution data of phatom perturbations in LVWHs. The black lines correspond to the perturbation of a phatom scalar field in EBWH in the absence of LV.

with  $h^{\mu\nu} := g^{\mu\nu} + 2\tilde{\eta}b^\mu b^\nu$ . Similarly to the case studied above, let us we assume that the LV-matter coupling constant is related to the LV-gravity coupling constant through<sup>1</sup>  $\tilde{\eta} = \tilde{\xi}_2/2$ , such that

<sup>1</sup>The difference in the sign of the relation between the coupling constants arises from the distinct nature of the scalar field. Specifically, the coupling constants are related by  $\tilde{\eta} = \varepsilon\tilde{\xi}_2/2$ , where  $\varepsilon = -1$  for phantom scalar fields and  $\varepsilon = +1$  for canonical scalar fields.

$h^{\mu\nu} = g^{\mu\nu} + \tilde{\xi}_2 \mathbf{b}^\mu \mathbf{b}^\nu$ , or explicitly

$$h^{\mu\nu} = \begin{pmatrix} -(1 - 2M/r)^{-1} & 0 & 0 & 0 \\ 0 & \frac{(1 - 2M/r)}{1 + l_V} & 0 & 0 \\ 0 & 0 & 1/r^2 & 0 \\ 0 & 0 & 0 & 1/r^2 \sin^2 \theta \end{pmatrix} + \begin{pmatrix} 0 & 0 & 0 & 0 \\ 0 & \frac{l_V (1 - 2M/r)}{1 + l_V} & 0 & 0 \\ 0 & 0 & 0 & 0 \\ 0 & 0 & 0 & 0 \end{pmatrix} \\ = \begin{pmatrix} -(1 - 2M/r)^{-1} & 0 & 0 & 0 \\ 0 & (1 - 2M/r) & 0 & 0 \\ 0 & 0 & 1/r^2 & 0 \\ 0 & 0 & 0 & 1/r^2 \sin^2 \theta \end{pmatrix} = g_S^{\mu\nu}$$

where  $g_S^{\mu\nu}$  are the contravariant components of the Schwarzschild metric. Therefore, Eq. (6.3) can be written as  $\nabla_\mu (g_S^{\mu\nu} \nabla_\nu \Psi) = 0$ . It is important to point out that the covariant derivative  $\nabla$  is compatible to the spacetime metric  $g_{\mu\nu}$ , but as we shall see, it is possible to introduce a new covariant derivative,  $\overset{\circ}{\nabla}$ , such that it is compatible to the Schwarzschild metric, and therefore  $\overset{\circ}{\nabla}_\mu \overset{\circ}{\nabla}^\mu \Psi = 0$ . Consequently,

**Table 2.** Quasinormal frequencies computed via DI, 6th-order WKB and Prony methods.

$\ell$	$l_T$	Method	$\text{Re}[\omega]a$	$-\text{Im}[\omega]a$
0	-0.1	DI	0.649596	0.589163
		WKB	0.625512	0.637461
		Prony	0.650444	0.589189
	0	DI	0.681431	0.617870
		WKB	0.656042	0.668575
		Prony	0.681298	0.617775
	0.1	DI	0.718331	0.651175
		WKB	0.691529	0.704740
		Prony	0.718678	0.651793
1	-0.1	DI	1.499518	0.505049
		WKB	1.502996	0.508252
		Prony	1.499688	0.504922
	0	DI	1.572708	0.529700
		WKB	1.576355	0.533059
		Prony	1.572913	0.529558
	0.1	DI	1.657780	0.558353
		WKB	1.661624	0.561894
		Prony	1.658019	0.558185
2	-0.1	DI	2.428141	0.488810
		WKB	2.429726	0.487335
		Prony	2.428628	0.488545
	0	DI	2.546656	0.512668
		WKB	2.548319	0.511121
		Prony	2.547213	0.512359
	0.1	DI	2.684411	0.540400
		WKB	2.686164	0.538769
		Prony	2.685056	0.540030

the dynamics of the scalar field perturbation is absent of any trait of the LV parameter  $l_V$ . In order to introduce the covariant derivative compatible to the Schwarzschild metric we recall that

$$\nabla_\mu w^\nu = \overset{\circ}{\nabla}_\mu w^\nu + C^\nu{}_{\mu\alpha} w^\alpha, \quad (6.4)$$

where  $C^\nu{}_{\mu\alpha} = \Gamma^\nu{}_{\mu\alpha} - \overset{\circ}{\Gamma}^\nu{}_{\mu\alpha}$ , with  $\Gamma^\nu{}_{\mu\alpha}$  and  $\overset{\circ}{\Gamma}^\nu{}_{\mu\alpha}$  denoting the Levi-Civita connections of the metric  $g_{\mu\nu}$  and  $(g_S)_{\mu\nu}$ , respectively. Thus,

$$\begin{aligned} \nabla_\mu (g_S^{\mu\nu} \nabla_\nu \Psi) &= \overset{\circ}{\nabla}_\mu (g_S^{\mu\nu} \overset{\circ}{\nabla}_\nu \Psi) + C^\mu{}_{\mu\alpha} g_S^{\alpha\nu} \overset{\circ}{\nabla}_\nu \Psi \\ &= \overset{\circ}{\nabla}_\mu \overset{\circ}{\nabla}^\mu \Psi + C^\mu{}_{\mu\alpha} g_S^{\alpha\nu} \overset{\circ}{\nabla}_\nu \Psi, \end{aligned}$$

where we have used that  $\nabla_\mu \Psi = \overset{\circ}{\nabla}_\mu \Psi$ . Since  $\Gamma^\mu{}_{\mu\alpha} = \partial_\alpha (\log \sqrt{-g})$  and  $\overset{\circ}{\Gamma}^\mu{}_{\mu\alpha} = \partial_\alpha (\log \sqrt{-g_S})$ , with  $g_S$  being the determinant of the metric  $(g_S)_{\mu\nu}$ , it is straightforward to check that

$$C^\mu{}_{\mu\alpha} = 0, \quad (6.5)$$

and therefore the scalar field equation (6.3) reduces to the standard Klein-Gordon equation. The generalization of this result for scalar perturbations subjected to LV-matter couplings in general space-times of the system (6.1) is direct.

By assuming that the perturbations of a (free) scalar field, say  $\Psi$ , is subjected to LV-matter couplings with non-vanishing VEV bumblebee,  $\mathfrak{b}^\mu$ , and non-vanishing VEV antisymmetric rank-2 tensor,  $b^{\mu\nu}$ , its dynamics is determined by

$$\nabla_\mu (q^{\mu\nu} \nabla_\nu \Psi) = 0, \quad (6.6)$$

where  $q^{\mu\nu} := g_{LV}^{\mu\nu} + 2(\tilde{\eta} \mathfrak{b}^\mu \mathfrak{b}^\nu + \eta b^{\mu\alpha} b^\nu{}_\alpha)$  and  $g_{LV}^{\mu\nu}$  are the contravariant components of some metric influenced by the LV induced by  $\mathfrak{b}^\mu$  and  $b^{\mu\nu}$ . By assuming that the LV-matter couplings and the LV-gravity couplings are related by  $\tilde{\eta} = \tilde{\xi}_2/2$  and  $\eta = \xi_2/2$ , one obtains  $q^{\mu\nu} := g_{LV}^{\mu\nu} + \tilde{\xi}_2 \mathfrak{b}^\mu \mathfrak{b}^\nu + \xi_2 b^{\mu\alpha} b^\nu{}_\alpha$ . As we have seen, depending on the VEV configurations and on the structure of spacetime metric, the auxiliary metric  $q^{\mu\nu}$  can take the same form as a metric of GR, that is  $q^{\mu\nu} = g_{GR}^{\mu\nu}$ . Additionally, one can introduce a new covariant derivative,  $\overset{\circ}{\nabla}$ , compatible with the auxiliary metric, such that Eq. (6.6) becomes

$$\overset{\circ}{\nabla}_\mu \overset{\circ}{\nabla}^\mu \Psi + C^\mu{}_{\mu\alpha} g_{GR}^{\alpha\nu} \overset{\circ}{\nabla}_\nu \Psi = 0, \quad (6.7)$$

thus the vanishing of the latter term on the left-hand side implies that the scalar perturbation propagate on the spacetime metric as it was propagating in a GR background, that is, without any trait of LV. Since  $g_{GR}^{\alpha\nu} \overset{\circ}{\nabla}_\nu \Psi$  is, in general, non-vanishing, the condition for the scalar perturbation to satisfy the Klein-Gordon equation can be summarized as

$$C^\mu{}_{\mu\alpha} = \partial_\alpha \left[ \log \left( \frac{\sqrt{-g_{LV}}}{\sqrt{-q}} \right) \right] = 0, \quad (6.8)$$

where  $g_{LV}$  and  $q$  are the determinant of the metrics  $(g_{LV})_{\mu\nu}$  and  $q_{\mu\nu}$ , respectively. It follows that, if  $\log(\sqrt{-g_{LV}}/\sqrt{-q})$  is constant and  $q^{\mu\nu} = g_{GR}^{\mu\nu}$ , the scalar perturbations subjected to LV-matter couplings in the spacetime with LV behave identically to scalar perturbations in standard GR spacetime. Consequently, these perturbations do not experience the effects of LV.

One can check that the condition (6.8) is fulfilled for scalar perturbation  $\Psi_{LV}$  in LVWHs of case I. In this case, under a suitable change of coordinates, namely  $\rho = x/\sqrt{1+l_V}$ , the contravariant components of the spacetime metric and of the auxiliary metric become, respectively,

$$g_{LV}^{\mu\nu} = \text{diag}(-1, 1/(1+l_V), 1/(a^2 + \rho^2), 1/[(a^2 + \rho^2) \sin^2 \theta]), \quad (6.9)$$

$$q^{\mu\nu} = \text{diag}(-1, 1, 1/(a^2 + \rho^2), 1/[(a^2 + \rho^2) \sin^2 \theta]) = g_{EB}^{\mu\nu}, \quad (6.10)$$

hence  $\log(\sqrt{-g_{LV}}/\sqrt{-q}) = -\log(\sqrt{1+l_V})$  is constant, and therefore  $C^\mu{}_{\mu\alpha} = 0$ . As a result, the perturbations subjected to LV-matter couplings in the LVWHs of case I propagate as they were lying in EBWHs.

## 7 Conclusion

We have obtained tideless wormhole solutions supported by phantom scalar fields within a Lorentz-violating gravity framework, incorporating non-trivial couplings in the matter sector. Specifically, we assume that tensor fields with non-zero VEVs directly influence the dynamics of the scalar fields. We explore three distinct scenarios:

- Case I: Modifications arising from the VEV of the bumblebee field.
- Case II: Modifications arising from the VEV of a rank-2 tensor field.
- Case III: Modifications arising from the combined contributions of both fields.

Surprisingly, the three wormhole solutions obtained in this work exhibit a structure remarkably similar to the LVWHs previously found in the literature, which were derived considering non-minimal couplings to the Riemann tensor. However, the models presented here are generated by scalar fields without a self-interaction potential.

Remarkably, in Case III, the effective contributions of LV from the non-zero VEV of the bumblebee field and the non-zero VEV of the antisymmetric rank-2 tensor are additive, despite originating from fields with different natures ( $b^\mu$  has a spacelike norm, while  $b^{\mu\nu}$  has a timelike norm). Notably, when the LV parameters satisfy a specific configuration, namely  $l_V = l_T$ , the line element of the LVWH (see Eq. (3.34)) simplifies to that of the EB wormhole. Consequently, experiments focusing solely on spacetime curvature effects may not detect signatures of LV. Further investigation into these gravity frameworks, particularly with two tensor fields that spontaneously break Lorentz symmetry, is essential to determine whether more astrophysically relevant solutions, such as black holes, can accommodate distinct combinations of LV parameters.

A promising avenue for detecting imprints of LV lies in the analysis of perturbations within these spacetimes. Since the Lorentz-violating fields can, in principle, couple to independent canonical scalar fields, the investigation of how the dynamics of such scalar fields are influenced by LV effects and how it can be told apart from the dynamics of scalar fields minimally coupled to the spacetime metric is well-motivated. The role of the LV parameters in each of these scenario can be notably different, thus it is expected that they have distinct QNM spectra. We computed these spectra using three distinct methods: the DI method, the 6th-order WKB approximation, and the Prony method, finding excellent agreement among the results.

Concerning scalar fields minimally coupled to the spacetime metric, our analysis for the wormhole of case III reveals that the real part of the QNM frequencies decreases as the difference  $l_V - l_T$  increases, while the imaginary part increases as the difference increases. Consequently, scalar field perturbations are more damped at smaller values of  $l_V - l_T$ . Cases I and II can be obtained as particular limits of case III by considering  $l_T = 0$  and  $l_V = 0$ , respectively.

The analysis of scalar fields subjected to LV-matter couplings is subtler. Scalar fields coupled to a stationary spacelike background vector (bumblebee) field propagate in a spacetime where LV is spontaneously triggered by the same vector as they were in a GR background. We illustrate this intriguing behavior for perturbations in the wormhole of Case I. As a consequence, the QNM spectra of these scalar perturbations match those of the EB wormhole. Similarly, this also happens in the static, spherically symmetric vacuum black holes found in Einstein-bumblebee gravity [28].

Conversely, scalar perturbations coupled to Lorentz-violating fields in case II and case III are influenced by LV. Since the contribution from the bumblebee VEV trivializes in Case III, the perturbations in both cases follow the same dynamical equation. In these scenarios, the non-vanishing VEV of the antisymmetric rank-2 tensor alters the QNM spectra compared to the EB wormhole. Our analysis reveals that the real part of the QNM frequencies increases with  $l_T$ , while the imaginary part decreases (becoming more negative) as  $l_T$  increases. Consequently, the scalar field perturbations are more damped at higher values of  $l_T$ .

Our results demonstrate that the presence of couplings between tensor fields that spontaneously trigger Lorentz violation and matter fields can introduce new gravitational physics. This may manifest either through the emergence of UCOs or through modifications to the dynamical equations governing perturbations. The latter is particularly intriguing, as the anisotropies induced by LV may affect the radial stability of compact objects supported by matter distributions coupled to Lorentz-violating tensor fields. A detailed analysis of the radial stability of LVWHs is currently underway.

## A Methods to compute QNMs

In order to determine the QNM associated to the scalar perturbations there are several methods available in the literature, either considering the time domain or considering the frequency domain. Here we present the methods we use in our analysis.

### A.1 Time domain integration and Prony method

Without assuming the temporal dependence  $\exp(-i\omega t)$  in the phantom perturbation decomposition (4.3), the equation for the perturbation becomes

$$\left( \frac{\partial^2}{\partial t^2} - \frac{\partial^2}{\partial x^2} + V_\ell \right) \psi(t, x) = 0, \quad (\text{A.1})$$

where  $V_\ell$  for  $\psi_g$  and  $\psi_{LV}$  is given by

$$V_\ell^g = \frac{(1 + l_V - l_T)(1 + \ell(\ell + 1)(1 + l_V - l_T))a^2 + \ell(\ell + 1)x^2}{(a^2(1 + l_V - l_T) + x^2)^2}, \quad (\text{A.2})$$

$$V_\ell^{LV} = \frac{-a^2(l_T - 1)(\ell^2 + \ell + 1) + \ell(\ell + 1)x^2}{(x^2 - a^2(l_T - 1))^2}, \quad (\text{A.3})$$

respectively. Equation (A.1) can be integrated following the Gundlach-Price-Pullin discretization scheme [58]. This involves introducing light-cone coordinates, specifically  $v \equiv t + x$  and  $u \equiv t - x$ . Thus, the wave equation can be expressed as

$$\left( 4 \frac{\partial^2}{\partial u \partial v} + V_\ell \right) \psi = 0. \quad (\text{A.4})$$

The numerical integration is then performed on a null grid which leads to the following expression for the discretized scalar field evolution

$$\psi_N = \psi_E + \psi_W - \psi_S - \frac{h^2}{8} V_\ell(S) (\psi_W + \psi_E) + O(h^4), \quad (\text{A.5})$$

where  $h$  is the stepsize between two neighboring grid points and subscripts indicate the point in the grid where the function is evaluated. Explicitly,  $S = (u, v)$ ,  $W = (u + h, v)$ ,  $E = (u, v + h)$  and

$N = (u + h, v + h)$ . As initial conditions for the scalar perturbation we use a Gaussian distribution on the  $u = 0$  surface, together with a constant profile on the  $v = 0$  surface, i.e.:

$$\psi(0, v) = \mathcal{I} e^{-(v-v_c)^2/2\sigma^2}, \quad (\text{A.6})$$

with height  $\mathcal{I} = 1$ , width  $\sigma^2 = 1$  and centered at  $v_c = 5$ . The temporal evolution data can be divided into three distinct stages: (i) an initial prompt response, heavily influenced by the selected initial conditions of the field; (ii) an exponential decay during intermediate times, governed by the QNMs; and (iii) a power-law decline at late times, resulting from the backscattering of the field in the tail of the potential [59].

In order to extract the QNM frequencies from the time-profile data we use the Prony method [60]. This method consists in the fitting of data through a linear combination of exponentials. Thus, the temporal evolution data can be expanded as

$$\psi(t) = \sum_{j=0}^p C_j \exp(-i\omega_j t), \quad (\text{A.7})$$

where  $C_j$  are complex coefficients and we consider solely the damped oscillation part of the signal, say from  $t_0$  to  $t = t_0 + 2p\Delta t$ , where  $\Delta t$  is the time interval of each point, and  $2p \in \mathbb{Z}$  is the number of sample signals. Hence, the temporal evolution data can be written as

$$\psi_n = \sum_{j=0}^p D_j z_j^n, \quad (\text{A.8})$$

where  $\psi_n = \psi(t_0 + nh)$ ,  $D_j = \exp(-i\omega_j t_0) C_j$ , and  $z_j = \exp(-i\omega_j \Delta t)$ . The core of the Prony method is to recognize that the above equation is the solution to some homogeneous linear constant-coefficient difference equation [60]. Thus, it is convenient to introduce the polynomial

$$P(z) = \prod_{k=1}^p (z - z_k) = \sum_{j=0}^p \alpha_j z^{p-j}, \quad (\text{A.9})$$

that by construction, has the  $z_k$  as its roots. Since  $\forall j, 1 \leq j \leq p, P(z_j) = 0$ , hence it follows that

$$\sum_{i=0}^p \alpha_i \psi_{j-i} = \sum_{i=0}^p \alpha_i \sum_{k=1}^p D_k z_k^{j-i} = \sum_{k=1}^p D_k z_k^{j-p} (z_k) = 0. \quad (\text{A.10})$$

By taking  $\alpha_0 = 1$ , the above equation becomes

$$\sum_{k=1}^p \alpha_k \psi_{j-k} = -\psi_j. \quad (\text{A.11})$$

Taking  $j$  from  $p + 1$  to  $2p$  we get  $p$  equations, and therefore we can find the  $\alpha_k$  coefficients. Once obtained these coefficients we can obtain the roots  $z_k$  by substituting  $\alpha_k$  into Eq. (A.9). The quasi-normal frequencies are therefore obtained by the relation  $\omega_k = \frac{i}{\Delta t} \log(z_k)$ , while the amplitudes  $D_j$  are obtained by inverting Eq. (A.8).

## A.2 Direct integration

In order to determine the QNM frequencies, one can solve directly the radial equations of the phantom perturbation. The DI is based on the shooting method and numerical root finding to obtain frequencies in the complex domain [61]. We divide the space at some value  $-\infty < x_m < \infty$ , then we integrate Eq. (4.11) from plus (minus) infinity backward (inward) to  $x_m$ , subjected to the corresponding boundary conditions, obtaining two solutions, respectively,  $\phi_{\pm}$ . The condition for the quasinormal modes is the vanishing of the Wronskian of the two solutions in the matching point, namely

$$(\psi_+\psi'_- - \psi_-\psi'_+)|_{x_m} = 0. \quad (\text{A.12})$$

The quasinormal frequencies are found as the roots of the above condition, where one can use standard root-finding algorithm, such as Newton's method.

To enhance the convergence, we write the solution of the radial equation at both infinities as a power series, respectively

$$\psi(x \rightarrow \pm\infty) = \exp(\pm i\omega x) \sum_{i=0}^N \frac{h_i^{\pm}}{x^i}, \quad (\text{A.13})$$

where  $h_i^{\pm}$  are the expansion coefficients and  $N$  is the order of the expansion. The coefficients are determined by plugging Eq. (A.13) in the differential equation for the radial part of the corresponding scalar field. We use Eq. (A.13) and its first-order derivative as boundary conditions to integrate Eq. (4.11). In our numerical calculations, without loss of generality, we set  $h_0^{\pm} = 1$ , additionally we use  $N = 20$ .

## A.3 WKB

Schrödinger-like equations, such as Eq. (4.5), are suitably solved using the Wentzel-Kramers-Brillouin (WKB) method if the effective potential  $U_{\omega\ell}$  has a single peak, located at  $x = x_0$ , and approaches constant (negative) values as  $x \rightarrow \pm\infty$  [62], which is indeed the case of the potential of the phantom perturbations studied here. The WKB method is based on the matching of the solutions of Eq. (4.5) as  $x \rightarrow \pm\infty$ , with the Taylor expansion around the peak of the effective potential at the zeroes of  $U_{\omega\ell}$  (turning points). From this approach follows the WKB rule

$$\frac{iU_{\omega\ell}(x_0)}{\sqrt{2U_{\omega\ell}''(x_0)}} - \sum_{j=2}^N \Lambda_j = n + \frac{1}{2}, \quad (\text{A.14})$$

where  $n$  labels the overtones, with  $n = 0$  being the fundamental mode, and  $\Lambda_j$  correction terms that depends on higher order derivatives of  $U_{\omega\ell}$  evaluated at  $x_0$ . The first-order correction was derived in Ref. [63], while higher-order corrections were progressively developed: up to third order in Ref. [64], up to sixth order in Ref. [65], and up to thirteenth order in Ref. [66]. In this work, to validate our numerical results, we use a 6th-order WKB approximation, finding excellent agreement.

## Acknowledgments

The authors would like to acknowledge Fundação de Amparo à Pesquisa e ao Desenvolvimento Científico e Tecnológico do Maranhão (FAPEMA), Conselho Nacional de Desenvolvimento Científico e Tecnológico (CNPq), Coordenação de Aperfeiçoamento de Pessoal de Nível Superior (CAPES) – Finance Code 001, from Brazil, for partial financial support. R.B.M. is supported by CNPq/PDJ 151250/2024-3. L.A.L is supported by FAPEMA BPD- 08975/24.

## References

- [1] G. Bertone, D. Hooper, and J. Silk, Particle dark matter: Evidence, candidates and constraints, *Phys. Rept.* **405**, 279–390 (2005).
- [2] A. G. Riess, A. V. Filippenko, P. Challis, A. Clocchiatti, A. Diercks, P. M. Garnavich, R. L. Gilliland, C. J. Hogan, S. Jha, R. P. Kirshner, et al., Observational evidence from supernovae for an accelerating universe and a cosmological constant, *The astronomical journal* **116**(3), 1009 (1998).
- [3] S. W. Hawking and R. Penrose, The singularities of gravitational collapse and cosmology, *Proceedings of the Royal Society of London. A. Mathematical and Physical Sciences* **314**(1519), 529–548 (1970).
- [4] C. Rovelli, *Quantum gravity*, Cambridge university press, 2004.
- [5] S. Weinstein and D. Rickles, *Quantum gravity*, (2005).
- [6] M. B. Green, J. H. Schwarz, and E. Witten, *Superstring theory*, volume 2, Cambridge University Press, 2012.
- [7] D. J. Gross, J. A. Harvey, E. Martinec, and R. Ryan, Heterotic string theory (I). The free heterotic string, in *Current Physics—Sources and Comments*, volume 4, pages 76–107, Elsevier, 1989.
- [8] A. Ashtekar, New Hamiltonian formulation of general relativity, *Physical Review D* **36**(6), 1587 (1987).
- [9] C. Rovelli and L. Smolin, Loop space representation of quantum general relativity, *Nuclear Physics B* **331**(1), 80–152 (1990).
- [10] J. Ambjørn, J. Jurkiewicz, and R. Loll, Emergence of a 4D world from causal quantum gravity, *Physical review letters* **93**(13), 131301 (2004).
- [11] P. Hořava, Quantum gravity at a Lifshitz point, *Physical Review D—Particles, Fields, Gravitation, and Cosmology* **79**(8), 084008 (2009).
- [12] S. Weinberg, Effective field theory, past and future, *International Journal of Modern Physics A* **31**(06), 1630007 (2016).
- [13] V. A. Kostelecký and S. Samuel, Spontaneous breaking of Lorentz symmetry in string theory, *Physical Review D* **39**(2), 683 (1989).
- [14] S. Liberati, Tests of Lorentz invariance: a 2013 update, *Classical and Quantum Gravity* **30**(13), 133001 (2013).
- [15] V. A. Kostelecký and R. Potting, CPT, strings, and meson factories, *Physical Review D* **51**(7), 3923 (1995).
- [16] V. A. Kostelecký and S. Samuel, Phenomenological gravitational constraints on strings and higher-dimensional theories, *Physical Review Letters* **63**(3), 224 (1989).
- [17] V. A. Kostelecký, Gravity, Lorentz violation, and the standard model, *Phys. Rev. D* **69**, 105009 (2004).
- [18] D. Colladay and V. A. Kostelecký, CPT violation and the standard model, *Physical Review D* **55**(11), 6760 (1997).
- [19] R. Bluhm, S.-H. Fung, and V. A. Kostelecký, Spontaneous Lorentz and Diffeomorphism Violation, Massive Modes, and Gravity, *Phys. Rev. D* **77**, 065020 (2008).
- [20] Q. G. Bailey and V. A. Kostelecký, Signals for Lorentz violation in post-Newtonian gravity, *Physical Review D—Particles, Fields, Gravitation, and Cosmology* **74**(4), 045001 (2006).
- [21] D. Capelo and J. Páramos, Cosmological implications of Bumblebee vector models, *Physical Review D* **91**(10), 104007 (2015).
- [22] R. Maluf, V. Santos, W. Cruz, and C. Almeida, Matter-gravity scattering in the presence of spontaneous Lorentz violation, *Physical Review D—Particles, Fields, Gravitation, and Cosmology* **88**(2), 025005 (2013).

- [23] R. Maluf, C. Almeida, R. Casana, and M. Ferreira Jr, Einstein-Hilbert graviton modes modified by the Lorentz-violating bumblebee field, *Physical Review D* **90**(2), 025007 (2014).
- [24] L. A. Lessa and J. E. G. Silva, Einstein-Bumblebee-dilaton black hole solution, *Eur. Phys. J. C* **83**(11), 1035 (2023).
- [25] R. Maluf and J. C. Neves, Black holes with a cosmological constant in bumblebee gravity, *Physical Review D* **103**(4), 044002 (2021).
- [26] B. Altschul, Q. G. Bailey, and V. A. Kostelecky, Lorentz violation with an antisymmetric tensor, *Phys. Rev. D* **81**, 065028 (2010).
- [27] M. Kalb and P. Ramond, Classical direct interstring action, *Physical Review D* **9**(8), 2273 (1974).
- [28] R. Casana, A. Cavalcante, F. P. Poulis, and E. B. Santos, Exact Schwarzschild-like solution in a bumblebee gravity model, *Phys. Rev. D* **97**(10), 104001 (2018).
- [29] C. Ding, C. Liu, R. Casana, and A. Cavalcante, Exact Kerr-like solution and its shadow in a gravity model with spontaneous Lorentz symmetry breaking, *Eur. Phys. J. C* **80**(3), 178 (2020).
- [30] R. V. Maluf and J. C. S. Neves, Black holes with a cosmological constant in bumblebee gravity, *Phys. Rev. D* **103**(4), 044002 (2021).
- [31] K. Yang, Y.-Z. Chen, Z.-Q. Duan, and J.-Y. Zhao, Static and spherically symmetric black holes in gravity with a background Kalb-Ramond field, *Phys. Rev. D* **108**(12), 124004 (2023).
- [32] W. Liu, D. Wu, and J. Wang, Static neutral black holes in Kalb-Ramond gravity, *JCAP* **09**, 017 (2024).
- [33] L. A. Lessa, R. B. Magalhães, and M. M. F. Junior, On the self-consistency of compact objects in Lorentz-violating gravity theories, arXiv preprint arXiv:2505.01374 (2025).
- [34] J.-Z. Liu, W.-D. Guo, S.-W. Wei, and Y.-X. Liu, Charged spherically symmetric and slowly rotating charged black hole solutions in bumblebee gravity, *The European Physical Journal C* **85**(2), 145 (2025).
- [35] Z.-Q. Duan, J.-Y. Zhao, and K. Yang, Electrically charged black holes in gravity with a background Kalb-Ramond field, *The European Physical Journal C* **84**(8), 798 (2024).
- [36] A. Delhom, J. Nascimento, G. J. Olmo, A. Y. Petrov, and P. J. Porfírio, Radiative corrections in metric-affine bumblebee model, *Physics Letters B* **826**, 136932 (2022).
- [37] J. Nascimento, G. J. Olmo, A. Y. Petrov, and P. Porfírio, On metric-affine bumblebee model coupled to scalar matter, *Nuclear Physics B* **1004**, 116577 (2024).
- [38] L. Flamm, *Beiträge zur Einsteinschen gravitationstheorie*, Hirzel, 1916.
- [39] A. Einstein and N. Rosen, The particle problem in the general theory of relativity, *Physical Review* **48**(1), 73 (1935).
- [40] H. G. Ellis, Ether Flow through a Drainhole: A Particle Model in General Relativity, *Journal of Mathematical Physics* **14**, 104–118 (1973).
- [41] K. A. Bronnikov, Scalar-Tensor Theory and Scalar Charge, *Acta Phys. Polon. B* **4**, 251–266 (1973).
- [42] H. G. Ellis, The evolving, flowless drainhole: A nongravitating-particle model in general relativity theory, *General Relativity and Gravitation* **10**, 105–123 (1979).
- [43] R. R. Caldwell, M. Kamionkowski, and N. N. Weinberg, Phantom energy: dark energy with  $w < -1$  causes a cosmic doomsday, *Physical review letters* **91**(7), 071301 (2003).
- [44] T. M. C. Abbott et al., Dark Energy Survey: implications for cosmological expansion models from the final DES Baryon Acoustic Oscillation and Supernova data, (3 2025).
- [45] R. V. Maluf and C. R. Muniz, Exact solution for a traversable wormhole in a curvature-coupled antisymmetric background field, *Eur. Phys. J. C* **82**(5), 445 (2022).
- [46] R. B. Magalhães, L. A. Lessa, and M. M. Ferreira Jr, Wormholes in Lorentz-violating gravity, arXiv preprint arXiv:2505.07590 (2025).

- [47] R. Bluhm and V. A. Kostelecky, Spontaneous Lorentz violation, Nambu-Goldstone modes, and gravity, *Phys. Rev. D* **71**, 065008 (2005).
- [48] L. A. Lessa, J. E. G. Silva, and C. A. S. Almeida, The bumblebee field excitations in a cosmological braneworld, *EPL* **141**(2), 29001 (2023).
- [49] L. A. Lessa, J. E. G. Silva, R. V. Maluf, and C. A. S. Almeida, Modified black hole solution with a background Kalb–Ramond field, *Eur. Phys. J. C* **80**(4), 335 (2020).
- [50] R. B. Magalhães, A. S. Masó-Ferrando, F. Bombacigno, G. J. Olmo, and L. C. Crispino, Echoes from bounded universes, *Physical Review D* **110**(4), 044058 (2024).
- [51] J. L. Blázquez-Salcedo, X. Y. Chew, and J. Kunz, Scalar and Axial Quasinormal Modes of Massive Static Phantom Wormholes, *Physical Review D* **98**, 044035 (2018).
- [52] K. D. Kokkotas and B. G. Schmidt, Quasi-normal modes of stars and black holes, *Living Reviews in Relativity* **2**, 1–72 (1999).
- [53] E. Berti, V. Cardoso, and A. O. Starinets, Quasinormal modes of black holes and black branes, *Classical and Quantum Gravity* **26**(16), 163001 (2009).
- [54] J. L. Blázquez-Salcedo, X. Y. Chew, and J. Kunz, Scalar and axial quasinormal modes of massive static phantom wormholes, *Physical Review D* **98**(4), 044035 (2018).
- [55] R. Konoplya and A. Zhidenko, Wormholes versus black holes: quasinormal ringing at early and late times, *Journal of Cosmology and Astroparticle Physics* **2016**(12), 043 (2016).
- [56] R. Konoplya, How to tell the shape of a wormhole by its quasinormal modes, *Physics Letters B* **784**, 43–49 (2018).
- [57] K. A. Bronnikov, R. A. Konoplya, and T. D. Pappas, General parametrization of wormhole spacetimes and its application to shadows and quasinormal modes, *Physical Review D* **103**(12), 124062 (2021).
- [58] C. Gundlach, R. H. Price, and J. Pullin, Late-time behavior of stellar collapse and explosions. I. Linearized perturbations, *Physical Review D* **49**(2), 883 (1994).
- [59] W. Krivan, P. Laguna, and P. Papadopoulos, Dynamics of Scalar Fields in the Background of Rotating Black Holes, *Physical Review D* **54**, 4728–4734 (1996).
- [60] E. Berti, V. Cardoso, J. A. Gonzalez, and U. Sperhake, Mining information from binary black hole mergers: a comparison of estimation methods for complex exponentials in noise, *Physical Review D—Particles, Fields, Gravitation, and Cosmology* **75**(12), 124017 (2007).
- [61] R. A. Konoplya and A. Zhidenko, Quasinormal modes of black holes: From astrophysics to string theory, *Reviews of Modern Physics* **83**(3), 793–836 (2011).
- [62] R. A. Konoplya, A. Zhidenko, and A. F. Zinhailo, Higher Order WKB Formula for Quasinormal Modes and Grey-Body Factors: Recipes for Quick and Accurate Calculations, *Classical and Quantum Gravity* **36**, 155002 (2019).
- [63] B. F. Schutz and C. M. Will, Black Hole Normal Modes - A Semianalytic Approach, *The Astrophysical Journal* **291**, L33 (1985).
- [64] S. Iyer and C. M. Will, Black-Hole Normal Modes: A WKB Approach. I. Foundations and Application of a Higher-Order WKB Analysis of Potential-Barrier Scattering, *Physical Review D* **35**, 3621–3631 (1987).
- [65] R. A. Konoplya, Quasinormal Behavior of the  $D$ -Dimensional Schwarzschild Black Hole and the Higher Order WKB Approach, *Physical Review D* **68**, 024018 (2003).
- [66] J. Matyjasek and M. Opala, Quasinormal Modes of Black Holes: The Improved Semianalytic Approach, *Physical Review D* **96**, 024011 (2017).